New puzzle in muon g-2 anomaly and it's possible solution

by

Ahmad Ali

Department of Physics

Quaid-i-Azam University Islamabad, Pakistan
(2020-2023)

A THESIS SUBMITTED IN PARTIAL FULFILLMENT OF THE REQUIREMENTS FOR THE DEGREE OF MASTERS OF PHILOSOPHY IN PHYSICS AT THE QUAID-I-AZAM UNIVERSITY, ISLAMABAD 45320, PAKISTAN. NOVEMBER,2023.

RESEARCH COMPLETION CERTIFICATE

Certified that the research work contained in the thesis titled New puzzle in muon g-2 anomaly and it's possible solution has been carried out and completed by Mr. Ahmad Ali Roll No. 02182013024 under my supervision.

Supervised by:

_____

Prof. Dr. Mansoor Ur Rehman
Department of Physics
Quaid-i-Azam University Islamabad

Submitted through:

_____

Prof. Dr. Kashif Sabeeh
Chairperson
Department of Physics
Quaid-i-Azam University Islamabad

To my beloved parents

Acknowledgment

Dear readers,

I would like to express my sincere gratitude to all those who have contributed to the successful completion of my thesis. First and foremost, I would like to extend my heartfelt thanks to my supervisor, Dr. Mansoor Ur Rahman, for their tireless support, guidance and encouragement throughout my academic journey. Your unwavering dedication and invaluable insights have been instrumental in shaping my research and leading me to the successful completion of my thesis. I am also deeply thankful to my teacher, Dr. Jamil Aslam, for his exceptional knowledge, guidance and encouragement. His passion for teaching and dedication to his students have inspired me to pursue my academic and professional goals.

I would also like to acknowledge the efforts of my great friend Muhammad Riyaz, who has been a constant source of support and encouragement. His contributions have been invaluable and have helped me to overcome any challenges that I faced during my research.

My friends and family have also played a crucial role in my academic journey, and I am grateful for their constant love and support, which has given me the strength to overcome any obstacles that I have encountered along the way.

Lastly, I would like to express my gratitude to all those who have directly or indirectly contributed to my thesis and this journey, for without their support, this achievement would not have been possible.

Sincerely, Ahmad Ali.

Contents

List of Figures

Abstract

Recently, the measurement of the muon $g-2$ at Fermilab has reconfirmed an earlier result by Brookhaven and revealed a perplexing discrepancy between the prediction of the Standard Model (SM) and the experimental results. The main factor contributing to the discrepancy is the hadronic vacuum polarization (HVP), and resolving this difference is crucial. However, the low-energy data from the cross-section of $e^+e^- \longrightarrow$ hadrons, which is used to calculate HVP, is in conflict with a recent result from the BMW collaboration using lattice QCD. This conflict is referred to as the "new muon $g-2$ puzzle." In this thesis, the suggestion is made that new physics (NP) could impact the cross-section of the process $e^+e^- \longrightarrow$ hadrons as a possible resolution to the new muon $g-2$ puzzle. Nevertheless, we demonstrate that this proposed solution is ruled out by several experimental limitations.

Chapter 1

Introduction

The circulating and spinning charged particle produce a magnetic field like magnetic dipole due to which it cause motion in a magnetic field to align with it called magnetic moment of charged particle. The relation between the orbital angular momentum ($\vec{L} = m\overrightarrow{r} \times \vec{v}$) and orbital magnetic moment $\overrightarrow{\mu_l}$ for a particle with mass m, charge q, and velocity $\overrightarrow{v}$ is given by, $\vec{\mu_l} = \frac{q}{2mc}\vec{L}$. The magnetic moment is also associated with particles have intrinsic spin. the mathematical relation is given by, $\vec{\mu_s} = g\frac{q}{2mc}\vec{S}$, The symbol "$g$" represents the gyromagnetic ratio. The gyromagnetic ratio "g" was predicted by Dirac to be equal to 2 for electrons and any other spin1/2 elementary particles in 1928 [1]. With the advancement of quantum electrodynamics (QED), it was discovered that the gyromagnetic ratio "g" differs from 2 by an amount of $2a_l$, where a_l is known as the magnetic moment anomaly, meaning that $g = 2(1 + a_l)$, and the anomaly can be represented as $a_l = \frac{g-2}{2}$ [1]. The cause of this anomaly is the result of radiative corrections, where the connection between an elementary particle and a photon is altered as a result of interactions with virtual particles. The value of "g" is effected by these quantum fluctuations, which increase the initial prediction of $g = 2$, as a result of interactions with virtual particles. In 1948, J. Schwinger carried out the initial calculation of the correction using quantum electrodynamics (QED) and found that "g" was increased by precisely α/π [17].

The SM in particle physics, which is based on a combination of the theory of relativity and quantum field theory with specific gauge symmetries $SU(3)_c \otimes SU(2)_L \otimes U(1)_Y$, has been very successful in explaining the interactions between all known fundamental particles with regards to electromagnetism, weak, and strong forces. Recently, the Fermi National Accelerator Laboratory's $g_\mu - 2$ Collaboration published their results of a precise measurement of the a_μ [2]. This measurement, in conjunction with a previous 2006 measurement from Brookhaven National Laboratory [3], shows a 4.2 standard deviation

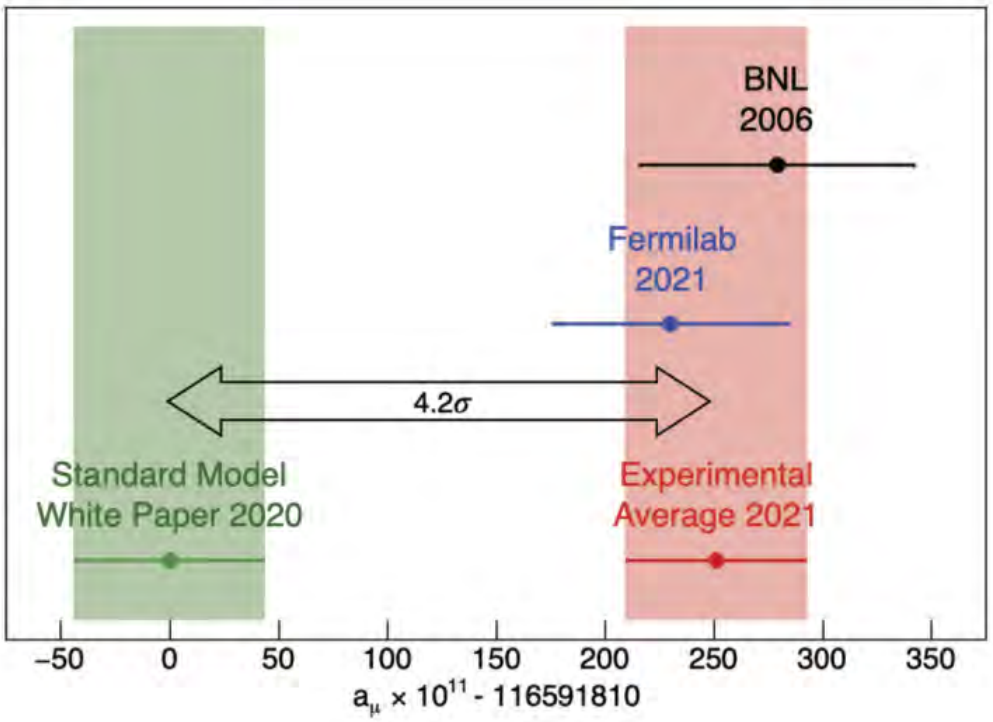

Figure 1.0.1: The difference between the experimental values and theoretical predictions of a_μ[1].

from the prediction made by the SM [4, 5].

$$\Delta a_\mu \equiv a_\mu^{Exp} - a_\mu^{SM} = (251 \pm 59) \times 10^{-11}. \tag{1.0.1}$$

such a deviation will indicate the presence of NP beyond the SM. Numerous theoretical papers have previously been published in an effort to explain this anomaly by NP.

The major source of uncertainty in the SM prediction for a_μ (referred to as a_μ^{SM} in Eq. (1.0.1) in the hadronic sector. These effects have been extensively studied in recent years. The a_μ^{SM} value is determined using the contribution to the $g_\mu - 2$ from hadronic vacuum polarization (HVP), obtained from the low-energy $e^+e^- \longrightarrow$ hadrons data, which is provided by the $g_\mu - 2$ theory initiative (TI) [6]. As an alternative, a first-principle lattice QCD method has been used to calculate the HVP contribution [6][7]. The leading HVP contribution to the $g_\mu - 2$ was recently calculated with sub-percent precision by the BMW lattice QCD collaboration (BMWc), finding a value, $(a_\mu^{HVP})^{BMW}$, which is greater then $(a_\mu^{HVP})^{TI}_{e^+e^-}$[8]. If the $(a_\mu^{HVP})^{BMW}$ is utilized to calculate a_μ^{SM} instead of $(a_\mu^{HVP})^{TI}_{e^+e^-}$,

the discrepancy with experimental results is reduced to 1.6σ. The results are as follows:

$$(a_\mu^{HVP})_{e^+e^-}^{TI} = 6931(40) \times 10^{-11}, \tag{1.0.2}$$

$$(a_\mu^{HVP})^{BMW} = 7075(55) \times 10^{-11}. \tag{1.0.3}$$

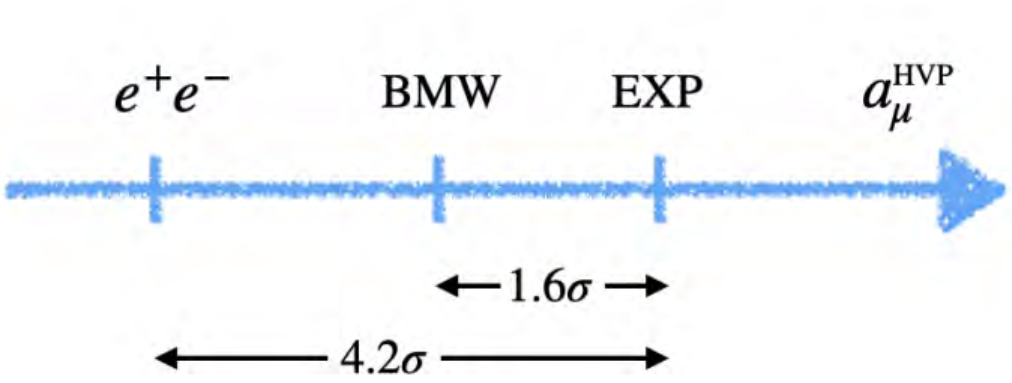

Figure 1.0.2: Comparison of the $(a_\mu^{HVP})_{e^+e^-}^{TI}$,$(a_\mu^{HVP})^{BMW}$ and $(a_\mu^{HVP})^{EXP}$[9].

Fig. 1.0.2 present an illustration of the current situation related to the leading HVP to the $g_\mu - 2$, where $(a_\mu^{HVP})^{EXP}$match with a_μ^{EXP}without assuming any NP. Hereafter, In Fig. 1.0.2 the discrepancy between $(a_\mu^{HVP})_{e^+e^-}^{TI}$ and $(a_\mu^{HVP})^{BMW}$will be referred to as the new $g_\mu - 2$ puzzle.

Assuming that $(a_\mu^{HVP})_{e^+e^-}^{TI}$ and $(a_\mu^{HVP})^{BMW}$ both are correct, the new $g_\mu - 2$ puzzle can be resolved by the introduction of NP effects that reconcile $(a_\mu^{HVP})_{e^+e^-}^{TI}$ and $(a_\mu^{HVP})^{BMW}$ without affecting the existing 1.6σ agreement between $(a_\mu^{HVP})^{BMW}$ and $(a_\mu^{HVP})^{EXP}$. Note that a direct NP contribution to $\triangle a_\mu$ will not solve the puzzle. To resolve the new $g_\mu - 2$ puzzle, we propose NP that modifies the cross-section σ_{had} of the $e^+e^- \rightarrow$hadrons process.

Chapter 2

Standard Model of Particle Physics

2.1 Standard Model

All of nature arises from a few basic components called fundamental particles, These particles interact with each other in only a limited number of ways. Physicists in the seventies developed a series of equations to describe these interactions and particles, resulting in a succinct theory known as the standard model of particle physics. The hypothetical particles that make up dark matter, those that convey gravity, and an explanation for the mass of neutrinos are noticeably absent from the standard model, yet it still provides a very realistic picture of practically all other observed events. The common visualization shows in Fig. 2.1.1.

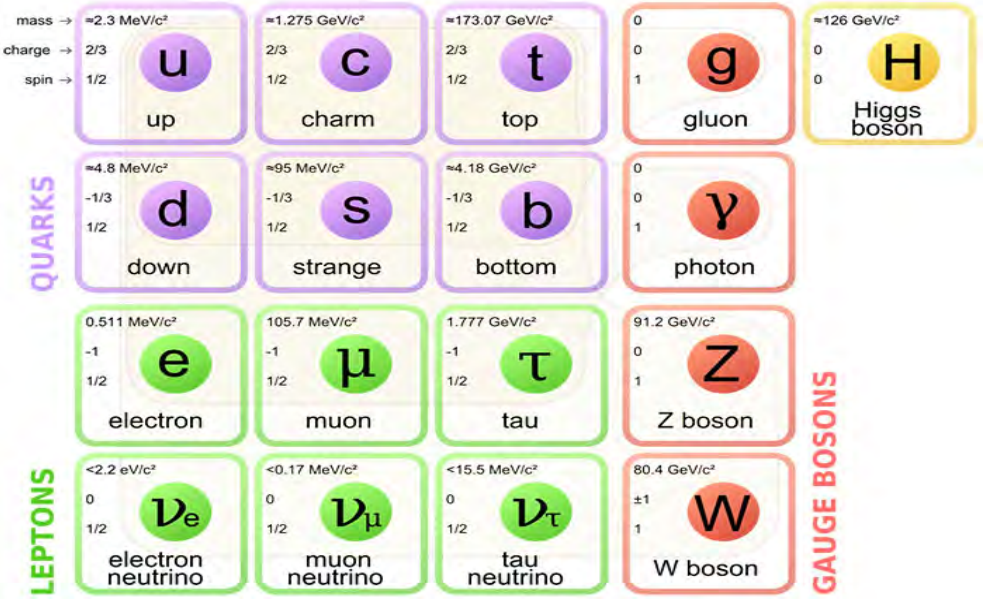

Figure 2.1.1: Concluded summary of the SM of particle physics [61].

Leptons and quarks are the two major types of matter particles. Keep in mind that there is an antimatter particle for every type of matter particle seen in nature. These particles have the same mass but are dissimilar in every other way [10].

2.1.1 Quarks

Let's begin by discussing quarks, focusing on the two varieties that compose protons and neutrons in atomic nuclei. These are the up quark, which has a charge of two-thirds of a unit of electric charge on electron (same charge on the charm and top quarks), and the down quark, which has a charge of -1/3 (same charge on the strange and bottom quarks). There are total six quarks (u, d, c, s, t, b) there respective properties given in Fig. 2.1.1. Additionally, quarks have a type of charge known as color. A quark's color charge can be either red, green, or blue. The quark is sensitive to the strong force because of its color. Quarks change their color by absorbing or emitting gluons, which are the strong force's particle carriers [10].

2.1.2 Leptons

The other class of matter particles, known as leptons, are the electron, muon, and tau, each of which has an electric charge of -1, and their corresponding neutrinos, which have an electrical charge of zero. The issue is that each type of matter particle has three successively heavier but otherwise similar counterparts that exist for unidentified reasons. For instance, the charm and strange quarks are present alongside the up and down quarks, while the top and bottom quarks are heavier still. The same is true of the leptons. The muon and muon neutrino, as well as the tau and tau neutrino, are present in addition to the electron and electron neutrino. Keep in mind that the neutrinos have tiny masses that are unknown. Leptons appear in a table with their corresponding properties.

In the Fig. 2.1.1 the first column particle called the first generation particle, and second called the second generation, and the third column particle called the third generation particles.

2.1.3 Force Mediator and Higgs Boson

We are just talking about the fundamental bosons that operate as a force mediator between two particles. In fact, all matter particles—aside from neutrinos—have an electric charge. The electromagnetic force can be sensed by these particles because they have an electric charge. The electromagnetic force's messengers, photons, are exchanged be-

tween them in order to communicate. In our model, charged particles are connected by wavy lines to depict electromagnetic interactions. Be aware that these interactions merely cause the particles to experience a push or a pull rather than transforming them into one another. The weak force is a little trickier than we first suggested. Other than the electrically charged carriers of the weak force, the W^+ and W^- bosons, The Z boson, another neutral carrier of the weak force, exists as well. Z bosons can be absorbed or emitted by particles without causing identity changes. These "weak neutral interactions" just result in energy and momentum loss or gain, similar to electromagnetic interactions. Orange wavy lines serve as a visual representation of weak neutral interactions. It is no accident that the electromagnetic interactions and weak neutral interactions are very similar. The electroweak interaction, which was a single force in the early universe, is the source of both the weak and electromagnetic forces. Quarks glue together to form mesons and baryons due to strong force of madiater called gluon . There are eight different types of gluons.

It is thought that the Higgs boson, a subatomic particle, gives other particles mass [13]. Theorist Peter Higgs first put forward the idea in the 1960s, and tests at the Large Hadron Collider at CERN, the European Organization for Nuclear Research, later proved it to be true. Because it is a scalar boson, it has no electric charge and zero spin. In addition, it differs from all other particles in the standard model of particle physics in that it is the only one that has not been directly detected. Instead, the evidence for its existence came from how it affected other particles. Particles gain mass through a process known as the Higgs mechanism. It suggests that the entire cosmos is made up of a Higgs field, an energy field that penetrates all of space. When interacting with this field, particles gain mass. The particle connected to this field, the Higgs boson, is in charge of giving other particles mass. It was a significant achievement in particle physics when the Higgs boson was discovered since it proved the existence of the Higgs field and the process by which particles gain mass.

It was a significant achievement in particle physics when the Higgs boson was discovered since it proved the existence of the Higgs field and the process by which particles gain mass. On July 4, 2012, CERN announced the discovery of the Higgs boson, which marked a significant advancement in our knowledge of the universe [12].

2.2 Quantum Electrodynamics

Quantum Electrodynamics (QED) is the theory that describes the electromagnetic force, which is responsible for the interaction between electrically charged particles. It is a fundamental theory of the electromagnetic interaction, one of the four fundamental interactions

of nature. It is a Quantum Field Theory (QFT), which means that it describes the behavior of particles and their interactions at the quantum level. In QED, the electromagnetic force is mediated by virtual photons, which are particles that do not have a mass but have energy and momentum. These photons are exchanged between charged particles, causing them to interact. One of the most important predictions of QED is the phenomenon of vacuum polarization, which occurs when virtual particles (such as photons) are created and destroyed in the vacuum. This effect can cause the charge of a particle to be screened, or reduced, when it is surrounded by other charges. QED also predicts the Lamb shift, which is a small shift in the energy levels of hydrogen atoms caused by the interaction of the electron with virtual photons. This effect was first observed experimentally in 1947, and it provided strong evidence for the validity of QED.

QED predicts the a_μ, which is a small deviation from the value predicted by classical physics. This deviation is caused by the interaction of the muon with virtual photons in the vacuum, which is known as vacuum polarization. The predictions of QED for the value of a_μ have been confirmed to a high degree of accuracy through experiments. However, the measured value of the $g_\mu - 2$ is slightly different than the value predicted by QED, which is known as the $g_\mu - 2$ puzzle. This discrepancy could be due to NP beyond the SM. Many theories have been proposed to explain this discrepancy, such as the presence of new particles or new interactions. Currently, many experimental effort is going on to measure the $g_\mu - 2$ value with higher precision and to understand the origin of the discrepancy, such as Fermilab's $g_\mu - 2$ experiment. Some theories that include new particles or new interactions beyond the Standard Model, such as Super-symmetry, Grand Unification, and extra dimensions, predict a value that is closer to the measured value, which could provide a solution to the $g_\mu - 2$ puzzle [11].

2.3 Quantum Chromodynamics

Quantum Chromodynamics (QCD) is a fundamental theory that explains the strong nuclear force, which is responsible for binding protons and neutrons in the atomic nucleus. This theory describes one of the four fundamental interactions of nature and is a non-abelian gauge theory, where interactions are governed by non-abelian symmetry group and mediated by gauge bosons that transmit the strong force. These bosons are called gluons. Gluons are mass less, have zero charge and carry a color charge, which is a property that allows them to interact with quarks and anti-quarks. QCD is based on the idea that protons and neutrons are made up of smaller particles called quarks. These quarks are held together by the strong force, which is carried by gluons. The strong force is a

fundamental force of nature, and it is much stronger than the electromagnetic force or the weak force. QCD predicts that protons and neutrons are composed of three quarks, which are held together by the exchange of gluons. This is known as confinement, which is the phenomenon that quarks and gluons are always confined within protons and neutrons, and cannot be isolated as individual particles.

One of the most important predictions of QCD is asymptotic freedom, which states that the strong force between quarks becomes weaker as their separation increases, this allows for the existence of free quarks at high energy, but not at low energy. QCD also predicts the existence of other particles, such as mesons and baryons, which are composed of quarks and anti quarks or three quarks respectively [14].

2.4 Weak Interaction

The weak interaction, also known as the weak nuclear force, is one of the four fundamental interactions of nature, and it's responsible for certain types of radioactive decay, such as beta decay, and it also plays a role in the process of nuclear fusion in stars. In the standard model, it's described as an exchange of intermediate vector bosons, specifically the W and Z bosons. These bosons are responsible for the weak force, and they mediate the interactions between particles such as quarks and leptons, it's also responsible for neutrino oscillations and plays a crucial role in electroweak symmetry breaking, which gives particles mass through the Higgs mechanism [14].

2.5 Vector and Axial Coupling

Vector coupling occurs when two particles interact through the exchange of a force carrier, such as a photon in electromagnetism or a gluon in the strong force. In the case of the weak force, the force carrier is the Z particle. When two particles interact through vector coupling, their properties such as spin, charge are conserved, meaning that the total amount of these properties remains constant before and after the interaction. The weak force has both vector and axial-vector couplings, which describe how the weak force acts on particles with different spins. Vector coupling describes the interaction of particles with spin $-1/2$ such as quarks and leptons, while axial-vector coupling describes the interaction of particles with spin -1 such as the intermediate vector bosons. Weak axial coupling refers to the axial-vector coupling of the weak force, which describes how the weak force acts on particles with spin -1. The weak axial coupling is related to the weak charge of a particle, which determines its sensitivity to the weak force. Particles with a non-zero

weak charge can interact with the weak force through the exchange of intermediate vector bosons, such as the W and Z particles.

2.6 Lattice QCD

Lattice QCD (Quantum Chromodynamics) is a theoretical and computational approach for studying the strong interaction between quarks and gluons, which make up the protons and neutrons in atomic nuclei. It is a non-perturbative method that involves discretizing space-time into a lattice and using Monte Carlo simulations to calculate the properties of hadrons and other bound states of quarks and gluons. The results of lattice QCD calculations are compared with experimental data to validate and improve our understanding of the strong nuclear force and the structure of matter.

In lattice QCD, spacetime is discretion into a four-dimensional grid or lattice, with each point on the lattice representing a location in spacetime. The lattice is used as a regularization of the continuous spacetime, allowing us to perform numerical computations on a finite, discrete set of points.

2.7 Optical Theorem

The optical theorem in quantum field theory states that the imaginary part of the forward scattering amplitude is equal to the total cross section for the incoming particles to scatter into all possible final states. This theorem provides a relationship between the scattering amplitude and the total cross section and is a fundamental result in the study of particle interactions in high-energy physics. The theorem has applications in a variety of physical processes, including deep inelastic scattering and the calculation of total cross sections in particle colliders.

There are two matted to calculate theoretically the SM contribution to a_μ one of them is lattice QCD and the other is theory initiative (TI) matted, in theory initiative matted we use the optical theorem.

Chapter 3

Theoretical Calculation of Muon Anomaly and Comparison with Experimental Value

3.1 Magnet Moment of Muon due to Spin

Spin magnetic moment, also known as intrinsic magnetic moment, is a measure of the magnetic field produced by an object's intrinsic angular momentum or "spin." It arises from the magnetic properties of an object's constituent particles and is proportional to the magnitude of its spin. The spin magnetic moment of an object is independent of its orbital motion and is a fundamental property. The magnetic moment $\vec{\mu}$ of an elementary particle follows,

$$\vec{\mu} = g\frac{q}{2m}\vec{S}. \tag{3.1.1}$$

In this equation, the symbol "g" stands for the gyromagnetic ratio [1]. The main challenge is to determine the accurate value of "g".

3.1.1 Theoretical Approach by Dirac for Determining the Gyromagnetic Ratio of Electron

Dirac's theoretical approach to determining the gyromagnetic ratio of a lepton involved using his theory of quantum mechanics to calculate the relationship between the magnetic moment and the spin of the particle.

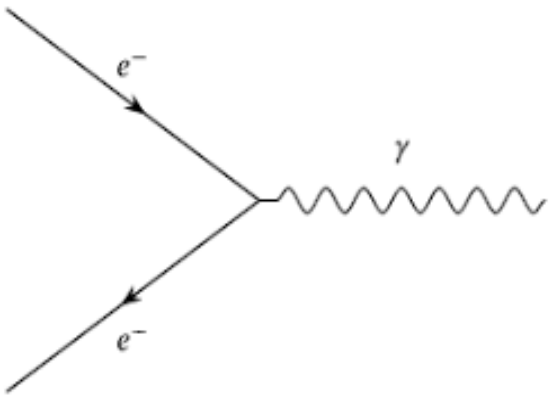

Figure 3.1.1: Tree level interaction of electron with external magnetic field [16].

In this part, Gaussian units (also known as Gaussian system of units, are a system of physical units based on the cgs system of units) are adopted. The Dirac equation is a first-order derivative form of the Schrodinger equation that takes into account special relativity and treats space and time symmetrically. The equation is derived from the relativistic energy-momentum relationship: $E^2 = (pc)^2 + (mc^2)^2$, leading to the expression of the Hamiltonian,

$$\mathcal{H} = \left((cp)^2 + \left(mc^2\right)\right)^{\frac{1}{2}}. \tag{3.1.2}$$

Dirac discovered a representation using a set of matrices that fulfill the following condition:

$$H = c\overrightarrow{\gamma} \cdot \overrightarrow{p} + \gamma^0 mc^2, \tag{3.1.3}$$

where,

$$\overrightarrow{\gamma} = \begin{pmatrix} 0 & \overrightarrow{\sigma}_i \\ \overrightarrow{\sigma}_i & 0 \end{pmatrix}, \quad \gamma^0 = \begin{pmatrix} I & 0 \\ 0 & -I \end{pmatrix}. \tag{3.1.4}$$

The 2×2 identity matrix is denoted as I and the Pauli spin matrices are represented byσ_i where i takes values $1, 2$ and 3. The Dirac equation is obtained by representing the variables E and $\overrightarrow{p}$ as operators: $\overrightarrow{p} \rightarrow \overrightarrow{P} = -i\hbar\overrightarrow{\nabla}$ and $E \rightarrow i\hbar\frac{\partial}{\partial t}$,

$$i\hbar\frac{\partial\psi(t)}{\partial t} = \left(c\overrightarrow{\gamma} \cdot \overrightarrow{P} + \gamma^0 mc^2\right)\psi(t), \tag{3.1.5}$$

where,

$$\psi(t) = \psi e^{-iEt/\hbar}. \tag{3.1.6}$$

Eq. (3.1.5) can be written more compactly as,

$$\left(i\hbar\gamma^{\mu}\partial_{\mu} - \gamma^{0}mc\right)\psi(t) \;\; = \;\; 0. \tag{3.1.7}$$

where,

$$\partial = \frac{1}{c}\frac{\partial}{\partial t} \text{ and } \partial_i = \frac{\partial}{\partial x^i}. \tag{3.1.8}$$

When there is a magnetic field described by the potential $A^{\mu} = (A^0, \overrightarrow{A})$, the Hamiltonian in Eq. (3.1.3) become,

$$H = c\left(\overrightarrow{\gamma}\cdot(\left(\overrightarrow{P} - q\overrightarrow{A}/c\right)\right) + \gamma^0 mc^2 + qA^0. \tag{3.1.9}$$

Eq. (3.1.5) implies,

$$i\hbar\frac{\partial\psi(t)}{\partial t} \;\; = \;\; \left(c\overrightarrow{\gamma}\cdot\overrightarrow{\pi} + \gamma^0 mc^2 + qA^0\right)\psi(t). \tag{3.1.10}$$

using Eq. (3.1.6),

$$E\psi \;\; = \;\; \left(c\overrightarrow{\gamma}\cdot\overrightarrow{\pi} + \gamma^0 mc^2 + qA^0\right)\psi(t), \tag{3.1.11}$$

where $\overrightarrow{\pi} = \overrightarrow{P} - q\overrightarrow{A}/c$.

And, the object ψ is composed of four components and can be expressed using two objects each having two components,

$$\psi \;\; = \;\; \begin{pmatrix}\chi\\ \Phi\end{pmatrix}, \tag{3.1.12}$$

Eq. (3.1.11) becomes,

$$\begin{pmatrix} E - mc^2 - qA^0 & -c\overrightarrow{\sigma}\cdot\overrightarrow{\pi} \\ -c\overrightarrow{\sigma}\cdot\overrightarrow{\pi} & E + mc^2 + qA^0 \end{pmatrix}\begin{pmatrix}\chi\\ \Phi\end{pmatrix} \;\; = \;\; \begin{pmatrix}0\\0\end{pmatrix}, \tag{3.1.13}$$

which implies,$\chi(E - mc^2 - qA^0) - c\Phi\overrightarrow{\sigma}\cdot\overrightarrow{\pi}$ $(E + mc^2 + qA^0)\Phi - (c\overrightarrow{\sigma}\cdot\overrightarrow{\pi})\chi$

$$(E - mc^2 - qA^0)\chi - c\overrightarrow{\sigma}\cdot\overrightarrow{\pi}\Phi \;\; = \;\; 0, \tag{3.1.14}$$

$$(E + mc^2 + qA^0)\Phi - (c\overrightarrow{\sigma}\cdot\overrightarrow{\pi})\chi \;\; = \;\; 0. \tag{3.1.15}$$

Eq. (3.1.15) gives,

$$\Phi = \left(\frac{c\,\overrightarrow{\sigma}\cdot\overrightarrow{\pi}}{(E+mc^2+qA^0)}\right)\chi, \tag{3.1.16}$$

When operating at slow speeds, the value of $E+mc^2$ is approximately equal to $2mc^2$, and as the energy from the field interaction is small compared to the rest mass, qA^0 is less than mc^2. The outcome is that,

$$\Phi \approx \left(\frac{\overrightarrow{\sigma}\cdot\overrightarrow{\pi}}{2mc+\frac{qA^0}{c}}\right)\chi, \tag{3.1.17}$$

$$\approx \frac{1}{2mc}\left(\overrightarrow{\sigma}\cdot\overrightarrow{\pi}\right)\left(1-\frac{qA^0}{2mc}\right)\chi. \tag{3.1.18}$$

Putting Eq. (3.1.18) in Eq. (3.1.14) the new equation is,

$$E'\chi = \left\{\frac{1}{2mc}(\overrightarrow{\sigma}.\overrightarrow{\pi})(\overrightarrow{\sigma}.\overrightarrow{\pi})\left(1-\frac{qA^0}{2mc}\right)+qA^0\right\}\chi, \tag{3.1.19}$$

where $E'=E-mc^2$. As we know the identity, $(\overrightarrow{\sigma}\cdot\overrightarrow{\alpha})(\overrightarrow{\sigma}\cdot\overrightarrow{\beta})=\overrightarrow{\alpha}\cdot\overrightarrow{\beta}+i\overrightarrow{\sigma}\cdot\overrightarrow{\alpha}\times\overrightarrow{\beta}$ and $\overrightarrow{\pi}\times\overrightarrow{\pi}=\frac{q}{c}\nabla(\overrightarrow{A}\cdot\overrightarrow{p})+\frac{q^2}{c^2}\overrightarrow{B}=\frac{iq\hbar}{c}\overrightarrow{B}$

This result can be obtained by using the left hand side to operate on a spinor Φ, utilizing the definition of $\overrightarrow{\pi}$, and remembering that $\overrightarrow{\nabla}\times\overrightarrow{A}=\overrightarrow{B}$,

$$\left\{\frac{\left(\overrightarrow{P}-q\overrightarrow{A}/c\right)^2}{2m}-\frac{q\hbar}{2mc}\overrightarrow{\sigma}\cdot\overrightarrow{B}+qA^0\right\}\chi = E'\chi. \tag{3.1.20}$$

The Hamiltonian is then,

$$H = \frac{\left(\overrightarrow{P}-q\overrightarrow{A}/c\right)^2}{2m}-\frac{q\hbar}{2mc}\overrightarrow{\sigma}\cdot\overrightarrow{B}+qA^0. \tag{3.1.21}$$

The term that describes the way in which the magnetic field and the magnetic moment of the spin interact is,

$$H = -\overrightarrow{\mu}\cdot\overrightarrow{B}=-g\frac{q\hbar}{2mc}\frac{\overrightarrow{\sigma}\cdot\overrightarrow{B}}{2}, \tag{3.1.22}$$

Comparing Eq. (3.1.21) to Eq. (3.1.22) leads to,

$$g = 2. \tag{3.1.23}$$

The above derivation follows sections of [16]. So, first, Dirac theoretically predicted g=2."

3.2 Anomaly in the Gyromagnetic Ratio

As Quantum Electrodynamics (QED) evolved, scientists made a remarkable discovery: the magnetic moment of fundamental particles, denoted by the symbol "g" does not precisely equal 2, as initially expected. Instead, it deviates from this value by a certain amount, symbolized as "$2a_l$," where "a_l" is termed the magnetic moment anomaly. In simpler terms, "a_l" quantifies how much "g" differs from the anticipated 2, and you can express this as the equation: $g = 2(1 + a_l)$. To calculate the anomaly, one can easily find it using the formula $a_l = (g - 2)/2$ [2]. But why does this anomaly even occur? The root cause lies in radiative corrections, which emerge due to interactions between elementary particles and virtual particles, particularly photons, within the quantum vacuum. These interactions cause changes in the way elementary particles relate to photons. Essentially, quantum fluctuations induced by these virtual particles influence the value of "g" causing it to deviate from the expected 2.

In 1948, physicist Julian Schwinger embarked on a groundbreaking journey by employing Quantum Electrodynamics to compute the magnitude of this correction. His work unveiled a precise increase in "g" by a specific fraction, α/π, with α representing the fine-structure constant. This finding underscores the profound impact of quantum fluctuations resulting from interactions with virtual particles on the magnetic moment of particles [17].

3.3 Theoretical Calculations of a_μ

The estimation of the a_μ within the SM framework is determined by adding up all the contributions from every component of the SM.

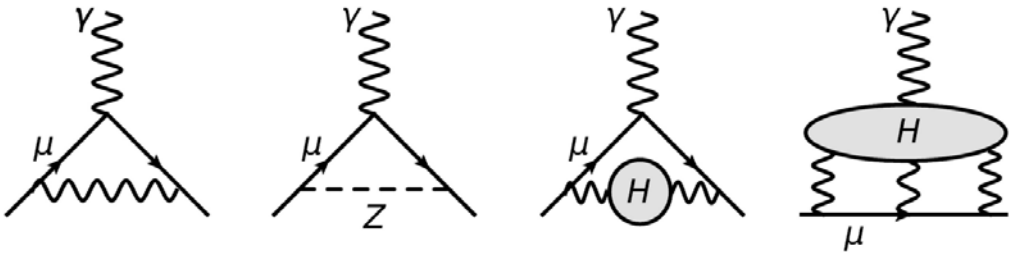

Figure 3.3.1: Different type of diagrams of SM particle contributions to a_μ [1].

$$a_\mu^{SM} \;=\; a_\mu^{QED} + a_\mu^{EW} + a_\mu^{HVP} + a_\mu^{HLBL}, \tag{3.3.1}$$

The anomaly a_μ include, a_μ^{QED} from electromagnetic interactions, a_μ^{EW} from electro-weak interactions, a_μ^{HVP} from hadronic vacuum polarization, and a_μ^{HLBL} from hadronic light-by-light (HLbL) scattering, Feynman diagram of such processes are shown in Fig. 3.3.1.

3.3.1 Quantum Electrodynamics Contributions

The anomaly a_μ^{QED} include all contributions from photons and leptons.

3.3.1.1 The Anomaly of a Charged Lepton from QED Beyond the Tree Level

Consider the class of diagrams ,

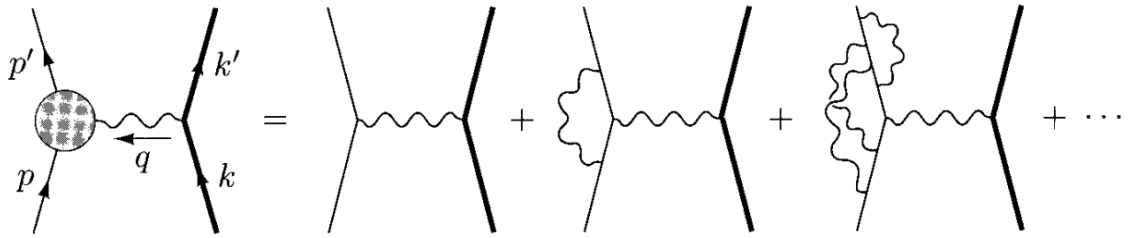

Figure 3.3.2: The circle indicated the sum of all amputed lowest-order electron-positron vertex corrections [18].

we will call this sum of vertex diagrams $-\iota e\Gamma^\mu$,

$$iM \;=\; \bar{u}(p')\Gamma^\mu u(p)\frac{i\eta^{\mu\nu}}{q^2}\bar{u}(k')ie\gamma_\mu u(k). \tag{3.3.2}$$

Our goal is to find Γ^μ is a function of $\gamma^\mu, p^\mu, p'^\mu, \not{p}, \not{p}', p^2, \not{p}^2$, where $(\not{p}, \not{p}', p^2, \not{p}^2)$, are Lorentz scalar. Using Dirac equation $\not{p}u(p) = m\,u(p)$, so $\Gamma^\mu\,(\gamma^\mu, p^\mu, p'^\mu, m, e)$.

$$\Gamma^\mu \;=\; \gamma^\mu A(p,p') + (p^\mu + p'^\mu)\,B(p,p') + (p'^\mu - p^\mu)\,C(p,p'). \tag{3.3.3}$$

Using ward identity $q_\mu\Gamma^\mu = 0$,

$$\not{q}(p,p')A + q(p,p')B + q\,(p'-p^\mu)\,C \;=\; 0, \qquad \text{where } q = p - p', \tag{3.3.4}$$

$$q \cdot (p + p') = (p - p')(p + p') = p'^2 - p^2 = m^2 - m^2 = 0. \tag{3.3.5}$$

it means that the coefficient of B is zero, and note that we will find all the values between $\bar{u}(p')$ and $u(p)$,

$$\begin{aligned} \bar{u}(p,p')\, \not{q}\, u(p,p') &= \bar{u}(p')(p' - p)\, u(p), & (3.3.6)\\ \bar{u}(p,p')\, \not{q}\, u(p,p') &= \bar{u}(p')(m - m)\, u(p), & (3.3.7)\\ \bar{u}(p,p')\, \not{q}\, u(p,p') &= 0. & (3.3.8) \end{aligned}$$

So first and second term is zero in the Eq. (3.3.3) which implies,

$$q \cdot (p - p') = -q^2 \Longrightarrow p + q = p'. \tag{3.3.9}$$

by squaring,

$$p^2 + q^2 + 2pq = p'^2 \implies q^2 + 2pq = 0. \tag{3.3.10}$$

if p, q is consider in rest frame of the incoming particle, then,

$$q^2 + 2pq = 0 \text{ this implies } C = 0, \tag{3.3.11}$$

so,

$$\Gamma^\mu = \gamma^\mu A + (p^\mu + p'^\mu)\, B. \tag{3.3.12}$$

Gordon identity,

$$\bar{u}(p')\gamma^\mu\, u(p) = \bar{u}(p') \left[\frac{P^\mu + P'^\mu}{2m} + \frac{i \sum^{\mu\nu} q_\nu}{2m} \right] u(p), \tag{3.3.13}$$

the second term in R.H.S gives,

$$\begin{aligned} \bar{u}(p') \frac{i \sum^{\mu\nu} q_\nu}{2m} u(p) &= \bar{u}(p) \left(\frac{i}{2m}\right) \left(\frac{i}{2}\right) \bar{u}(p') \left[\gamma^\mu . \gamma^\nu\right] (p'_\nu - p_\nu)\, u(p), & (3.3.14)\\ &= -\frac{1}{4m} \bar{u}(p') \left((\gamma^\mu \gamma^\nu - \gamma^\nu \gamma^\mu)\, p'_\nu - (\gamma^\mu \gamma^\nu - \gamma^\nu \gamma^\mu)\, p_\nu \right) u(p), \\ &= -\frac{1}{4m} \bar{u}(p') \left((2\eta^{\mu\nu} - 2\gamma^\nu \gamma^\mu)\, p'_\nu - (2\eta^{\mu\nu} - 2\gamma^\nu \gamma^\mu)\, p_\nu \right) u(p), \end{aligned}$$

Use identity to make $\not{p}'$and $\not{p}$ because we can find $\bar{u}(p')\not{p}$, and $\not{p}u(p)$, when we use Dirac

equation,

$$\bar{u}(p')\,\frac{i\sum^{\mu\nu}q_\nu}{2m}u(p) = -\frac{2}{4m}\bar{u}(p')\left[p'^{\mu}-m\gamma^{\mu}\right]-\left[m\gamma^{\mu}-p^{\mu}\right]u(p), \tag{3.3.15}$$

$$= -\frac{2}{4m}\bar{u}(p')\left[(p'^{\mu}+p^{\mu})-2m\gamma^{\mu}\right]u(p), \tag{3.3.16}$$

From Eq. (3.3.14) and Eq. (3.3.16) we have,

$$p'^{\mu}+p^{\mu} = \gamma^{\mu}-\frac{i\sum^{\mu\nu}q_\nu}{2m}, \tag{3.3.17}$$

put Eq. (3.3.17) in Eq. (3.3.12) we have,

$$\Gamma^{\mu}(p',p) = \gamma^{\mu}F_1(q^2)+\frac{i\sum^{\mu\nu}q_\nu}{2m}F_2(q^2), \tag{3.3.18}$$

$F_1(q^2)=A$ and $F_2(q^2)=B$ are called form factors, where, $F_1(q^2)=1$, and $F_2(q^2)=0$, for least order, $q\to 0$, lets start from the static potential, the external magnetic field,

$$\Delta H_{int} = \int d^3x\, eA^{cl}_{\mu}J^{\mu}, \quad \text{where } J^{\mu}=\bar{\psi}(x)\gamma^{\mu}\psi(x). \tag{3.3.19}$$

The Feynman amplitude will be given for this process,

$$iM(2\pi)\,\delta(p'_1-p_1) = -ie\bar{u}(p')\gamma^{\mu}u(p)A^{cl}_{\mu}(p'-p), \tag{3.3.20}$$

for all vertex convection $\gamma^{\mu}=\Gamma^{\mu}$, For static vector potential $A^{cl}_{\mu}(x)=(0,\,\vec{A})$,

$$iM = \left[\bar{u}(p')\left(\gamma^{i}F_1(q^2)\right)+\frac{i\sum^{i\nu}q_\nu}{2m}F_2(q^2)\right]u(P)\,\tilde{A^{i}_{cl}}(q), \tag{3.3.21}$$

$$u(k)=\frac{k+m}{\sqrt{2m\,(E+m)}}u(0)=\begin{pmatrix}\sqrt{\frac{(E+m)}{2m}}\phi(0),\\ \frac{\vec{\sigma}.\vec{k}}{\sqrt{2m(E+m)}}\phi(0)\end{pmatrix}, \tag{3.3.22}$$

according to Dirac equation, $\phi(0)$ is a two component spinor, when p, p' and q are so small as compared to mass of the electron.

As $V(x)=-<\vec{\mu}>\cdot\vec{B}(x)$. For static magnetic field the vector potential is, $A^{cl}_{\mu}(x)=\left(0,A(\vec{x})\right)$, $\left(\text{where, }\tilde{A}^{cl}_{\mu}(\vec{q})\text{ is the fourier transform of }A^{cl}_{\mu}(\text{x})\right)$,

$$iM = ie\bar{u}(p')\left[\gamma^{i}F_1(q^2)+i\frac{\sigma^{\mu\nu}}{2m}q_\nu F_2(q^2)\right]u(p)\tilde{A}^{cl}_{\mu}(\vec{q}), \tag{3.3.23}$$

$$u(k) = \frac{\not{k} + m}{\sqrt{2m\,(E+m)}} u(0) = \begin{pmatrix} \sqrt{\frac{(E+m)}{2m}}\phi(0) \\ \frac{\vec{\sigma}.\vec{k}}{\sqrt{2m(E+m)}}\phi(0) \end{pmatrix}, \tag{3.3.24}$$

for spin $1/2$, $\phi(0) = \begin{pmatrix} 1 \\ 0 \end{pmatrix}$, and for spin $-1/2$, $\phi(0) = \begin{pmatrix} 0 \\ 1 \end{pmatrix}$, and as we know $\gamma^0 = \begin{pmatrix} I & 0 \\ 0 & I \end{pmatrix}$, and $\gamma^i = \begin{pmatrix} 0 & \sigma^i \\ -\sigma^i & 0 \end{pmatrix}$, first of all we will compute the first term of Eq. (3.3.23),

$$\bar{u}(p')\gamma^i u(p) = u^\dagger(p')\gamma^0\gamma^i u(p) = u^\dagger(p') \begin{pmatrix} 0 & \sigma^i \\ -\sigma^i & 0 \end{pmatrix} u(p), \tag{3.3.25}$$

$$\begin{aligned} \overline{u}(p')\gamma' u(p) &= \begin{pmatrix} \phi'(0)\sqrt{\frac{E+m}{2m}} & \phi'(0) & \frac{\overrightarrow{\sigma}.\overrightarrow{p}'}{\sqrt{\frac{2m}{E+m}}} \end{pmatrix} \begin{pmatrix} 0 & \sigma^i \\ \sigma^j & 0 \end{pmatrix} \begin{pmatrix} \sqrt{\frac{E+m}{2m}}\phi(0) \\ \frac{\vec{\sigma}.\vec{k}}{\sqrt{\frac{2m}{E+m}}}\phi(0) \end{pmatrix} \\ &= \frac{1}{2m}\left(\sqrt{\frac{E+m}{E'+m}}\phi^{\dagger'}(0)\overrightarrow{\sigma}.\overrightarrow{p}'\sigma^j\phi(0) + \sqrt{\frac{E'+m}{E+m}}\phi^{\dagger'}(0)\sigma^j\overrightarrow{\sigma}.\overrightarrow{p}\,\phi(0) \right) \end{aligned} \tag{3.3.26}$$

for $E = E'$ in the non-relativistic term order of p^2,

$$\overline{u}(p')\gamma^j u(p) = \frac{1}{2m}(\phi^{\dagger'}(0)\overrightarrow{\sigma}.\overrightarrow{p}'\sigma^j\phi(0) + \phi^{\dagger'}(0)\sigma^j\overrightarrow{\sigma}.\overrightarrow{p}\,\phi(0)), \tag{3.3.27}$$

Using $\sigma^i\sigma^i = \delta^{ij} + i\epsilon^{ijk}\sigma^k$,

$$\begin{aligned} \bar{u}(p')\gamma^i u(p) &= \frac{1}{2m}\phi'^\dagger(0)\left(\sigma^i\sigma^i p'^j + \sigma^i\sigma^j p^j\right)\phi(0), & (3.3.28)\\ &= \frac{1}{2m}\phi'^\dagger(0)\left(p+p'\right)^i + i\epsilon^{ijk}\sigma^k\left(p'^j - p^j\right)\phi(0), & (3.3.29)\\ &= \phi'^\dagger(0)\left(-\frac{i}{2m}\epsilon^{ijk}q^i\sigma^k\right)\phi(0) + \cdots . & (3.3.30) \end{aligned}$$

Now compute the second term of Eq. (3.3.23),

$$\bar{u}(p')\sigma^{i\nu}q_\nu u(p) = \bar{u}(p')\Sigma^{ij}u(p) + \cdots, \text{ where } \Sigma^{ij} = \frac{i}{2}\left[\gamma^i,\gamma^j\right] = \epsilon^{ijk}\begin{pmatrix} \sigma^k & 0 \\ 0 & \sigma^k \end{pmatrix} \tag{3.3.31}$$

$$\frac{i}{2m}\bar{u}(p')\sigma^{i\nu}q_\nu u(p) = \frac{i}{2m}\bar{u}(p')\Sigma^{ij}q_j u(p) + \cdots , \tag{3.3.32}$$

$$= \frac{i}{2m}u^\dagger(p')\begin{pmatrix} I & 0 \\ 0 & I \end{pmatrix}\begin{pmatrix} \sigma^k & 0 \\ 0 & \sigma^k \end{pmatrix} u(p)\epsilon^{ijk} + \cdots . \tag{3.3.33}$$

where,

$$u(p) = \begin{pmatrix} \sqrt{\frac{(E+m)}{2m}}\phi(0), \\ \frac{\vec{\sigma}.\vec{p}}{\sqrt{2m(E+m)}}\phi(0) \end{pmatrix}, \text{ because the upper exponent is linear in} q, \text{ and } E = E' = m, \tag{3.3.34}$$

Eq. (3.3.33) implies,

$$\frac{i}{2m}\bar{u}(p')\sigma^{i\nu}q_\nu u(p) = \frac{i}{2m}\phi'^\dagger(o)\sqrt{\frac{(E+m)(E'+m)}{2m}}\sigma^k\phi(0)\epsilon^{ijk}(-q_j) + \cdots , \tag{3.3.35}$$

$\sqrt{\frac{(E+m)(E'+m)}{2m}}$=1,

$$\bar{u}(p')\sigma^{i\nu}q_\nu u(p) = \frac{-i}{2m}\phi'^\dagger(o)\sigma^k\phi(0)\epsilon^{ijk}(q_j) + \cdots . \tag{3.3.36}$$

Now substituting Eq. (3.3.30) and Eq. (3.3.33) in Eq. (3.3.23) (in the Feynman amplitude formula), which implies,

$$iM = -ie\,(2m)\,\phi'^\dagger(o)\left[-\frac{1}{2m}\sigma^k\,(F_1(0)+F_2(0))\right]\left(\phi(0)\left[i\epsilon^{ijk}q_j\tilde{A}^i_{cl}(\vec{q})\right]\right). \tag{3.3.37}$$

If, $\vec{B}(x) = \vec{\nabla}\times\vec{A}(x)$, then the Fourier transform of $\vec{B}(x)$, will be as,

$$B^k(q) = i\epsilon^{ijk}q_j\tilde{A}^i_{cl}(q), \tag{3.3.38}$$

$$iM = -ie(2m)\phi'^\dagger(0)\left[-\frac{1}{2m}\sigma^k\,(F_1(0)+F_2(0))\right]\left(\phi(0)\tilde{B}^k(q)\right), \tag{3.3.39}$$

$$V(x) = -<\bar{\mu}>\cdot\vec{B}(x), \tag{3.3.40}$$

$$<\bar{\mu}> = \frac{e}{2m}2\,[F_1(0)+F_2(0)]\,\phi'^\dagger(o)\frac{\sigma}{2}\phi(0), \tag{3.3.41}$$

as we know that $<\bar{\mu}>=\frac{e}{2m}g\vec{S}$,where $\vec{S} = \phi'^\dagger(o)\frac{\sigma}{2}\phi(0)$, and $g = 2\,[F_1(0)+F_2(0)]$, also

we know that $F_1(0) = 1$ so,

$$g = 2\left[1 + F_2(0)\right], \tag{3.3.42}$$

$$F(0) = \frac{g-2}{2}. \tag{3.3.43}$$

This calculation is followed [18].

The Electron Vertex Function: Evaluation

To calculate one-loop contribution to e^- vertex function,

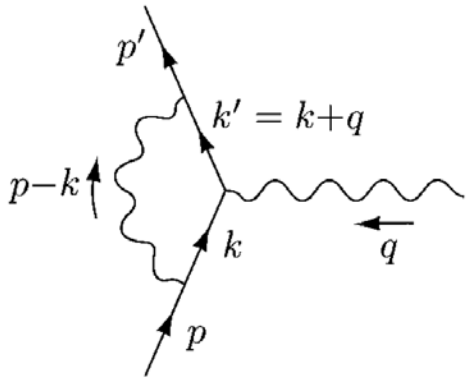

Figure 3.3.3: Feynman diagram of one-loop contribution to e^- vertex function [18].

Applying the Feynman rules we find that $\Gamma^\mu = \gamma^\mu + \delta\Gamma^\mu$ where,

$$\begin{aligned}
\bar{u}(p')\delta\Gamma^\mu u(p) &= \int \bar{u}(p')\frac{(ie\gamma^\nu)\, i\,(\not{k}+m)}{k'^2 - m^2 + i\epsilon}\gamma^\mu \frac{(\not{k}+m)}{k^2 - m^2 + i\epsilon}\,(ie\gamma^\rho)\,u(p)\frac{-i\eta}{(k-p)^2 + i\epsilon}\frac{d^4k}{(2\pi)^4}, \\
&= \int \frac{(i)(ie)^2(-i)u(p')\gamma^\nu\,(\not{k}+m)\,\gamma^\mu\,(\not{k}+m)\,\gamma_\nu\,u(p)}{(k'^2 - m^2 + i\epsilon)\,(k^2 - m^2 + i\epsilon)\left[(k-p)^2 + i\epsilon\right]}\frac{d^4k}{(2\pi)^4}, \qquad (3.3.44) \\
&= 2ie^2\int \frac{d^4k}{(2\pi)^4}\frac{u(p')\left[\not{k}\gamma^\mu\not{k}' + m^2\gamma^\mu - 2m\,(k+k')^\mu\right]u(p)}{\left[(k-p)^2 + i\epsilon\right](k'^2 - m^2 + i\epsilon)\,(k^2 - m^2 + i\epsilon)}, \qquad (3.3.45)
\end{aligned}$$

Feynman parametrization method to solve the integral,

$$\frac{1}{AB} = \int_0^1 \frac{dx}{\left[xA + (1-x)\,B\right]^2} = \int_0^1 \frac{dx}{\left[x\,(A-B) + B\right]^2}, \tag{3.3.46}$$

$let\, x(A-B)+B=t,$ then $dt=(A-B)\,dx,$

$$\frac{1}{AB}=\frac{1}{A\cdot B}\int_A^B\frac{dt}{t^2}=\int_0^1\frac{dx\,dy\delta(x+y-1)}{\left[xA+yB\right]^2}, \tag{3.3.47}$$

generally,

$$\frac{1}{A_1\cdot A_2\cdot A_3\cdots A_n} \;=\; \int_0^1\frac{dx_1dx_2dx_3\cdots dx_n\delta\left(\sum x_i-1\right)(n-1)!}{\left[x_1A_1+x_2A_2+x_3A_3+\cdots x_nA_n\right]^n}, \tag{3.3.48}$$

which implies,

$$\frac{1}{\left[(k-p)^2+i\epsilon\right]\left(k'^2-m^2+i\epsilon\right)\left(k^2-m^2+i\epsilon\right)} \;=\; \int_0^1 dxdydz\,\delta(x+y+z-1)\frac{1}{D^3},$$

where,

$$D=x\left(k^2-m^2\right)+y\left(k'^2-m^2\right)+z\left(k-p\right)^2+(x+y+z)\,i\epsilon, \tag{3.3.49}$$

as $x+y+z=1,\ k'^2=k^2+q^2+2k.q$ and $(k-p)^2=k^2+p^2-2k.p$ this implies,

$$\begin{aligned} D &= xk^2-xm^2+y\left(k^2+q^2+2k.q\right)-ym^2+z\left(k^2+p^2-2k.p\right)+i\epsilon, && (3.3.50)\\ &= k^2-2k.\left(yq-zp\right)+yq^2+zp^2-(x+y)\,m^2+i\epsilon, && (3.3.51)\end{aligned}$$

last expression depend on $k^2$and k we introduce a variable l so make it complete square.

Let,

$$l=k+yq-zp, \tag{3.3.52}$$

$$\begin{aligned} l^2 &= k^2+2k\cdot(yq-zp)+y^2q^2+z^2p^2-2yzp\cdot q, && (3.3.53)\\ l^2-D &= l^2-D=k^2+2k\cdot(yq-zp)+y^2q^2+z^2p^2-2yzp\cdot q && (3.3.54)\\ &\quad -\left(k^2+2k\cdot(yq-zp)\right)+yq^2+zp^2-(x-y)\,m^2+i\epsilon, && (3.3.55)\\ &= y\,(y-1)\,q^2+z\,(z-1)\,p^2-2yzp\cdot q-(x+y)\,m^2+i\epsilon, && (3.3.56)\end{aligned}$$

as $x+y+z=1\implies x+y=1-z$ and $y-1=-(x+z)$ implies,

$$\begin{aligned} l^2-D &= -y\,(x+z)\,q^2+z\,(z-1))\,m^2+(1-z)\,m^2-2yzp\cdot q+i\epsilon, && (3.3.57)\\ &= -y\,(x+z)\,q^2+z^2m^2-zm^2+m^2+zm^2-2yzp\cdot q+i\epsilon, && (3.3.58)\\ &= -y\,(x+z)\,q^2+(1-z)^2\,m^2-2yzp\cdot q+i\epsilon, && (3.3.59)\\ &= -yxq^2-yzq^2+((1-z)\,m^2-2yzp\cdot q+i\epsilon, && (3.3.60)\end{aligned}$$

using $q^2 + 2p \cdot q = 0$ so $p \cdot q = \frac{-q^2}{2}$ which implies,

$$\begin{aligned} l^2 - D &= -yxq^2 - yzq^2 + (1-z)^2 m^2 + yzq^2 + i\epsilon, && (3.3.61)\\ l^2 - D &= -yxq^2 + ((1-z) m^2 + i\epsilon, && (3.3.62)\\ l^2 - D &= -yxq^2 + ((1-z) m^2 + i\epsilon, && (3.3.63)\\ D &= -l^2 - yxq^2 + ((1-z) m^2 + i\epsilon, && (3.3.64)\\ D &= l^2 - \Delta + i\epsilon, && (3.3.65) \end{aligned}$$

where $\Delta \equiv -xyq^2 + (1-z)^2 m^2$.

Since the denominator is even function of l any integration of the form $\int \frac{d^4l}{(2\pi)^4} \frac{l^\mu}{D^3} = 0$, if $\mu \neq \nu$ it is also symmetric under the axiom of μ and ν, then symmetry require it must be proportional to $\eta^{\mu\nu}$,

$$\int \frac{d^4l}{(2\pi)^4} \frac{l^\mu l^\nu}{D^3} = 0, \text{ if } \mu \neq \nu, \quad (3.3.66)$$

this implies,

$$\int \frac{d^4l}{(2\pi)^4} \frac{l^\mu l^\nu}{D^3} = \int \frac{d^4l}{(2\pi)^4} \frac{\eta^{\mu\nu}}{D^3} \rho = \int \frac{d^4l}{(2\pi)^4} \frac{\eta^{\mu\nu}}{D^3} (\frac{1}{4} l^2), \quad (3.3.67)$$

we will use this formula ,to solve the integral of Eq. (3.3.45) we simplify the numerator of Eq. (3.3.45) first,

$$\begin{aligned} \text{nomerator} &= \bar{u}(p') \left[\not{k} \gamma^\mu \not{k}' + m^2 \gamma^\mu - 2m(k+k')^\mu \right] u(p), \quad k' = k + q, \text{ and } l = k + yq - zp,\\ &= \bar{u}(p') \left[(\not{l} - y\not{q} + 2\not{p}) \gamma^\mu (\not{l} + \not{q} - y\not{q} + z\not{p}) + m^2 \gamma^\mu - 2mq^\mu - 4m(l - yq + zp)^\mu \right] u(p),\\ &= \bar{u}(p') [\not{l} \gamma^\mu \not{l}^\nu + \not{l} \gamma^\mu (\not{l} - y\not{q} - z\not{p}) + (-y\not{q} + z\not{p}) \gamma^\mu \not{l} ((1-y)\not{q} + z\not{p}) + m^2 \gamma^\mu \quad (3.3.68)\\ &\quad -2m(q^\mu - 2yq^\mu - 2l^\mu + 2pz^\mu] u(p), \quad (3.3.69) \end{aligned}$$

The second term is in the form$\int d^n l \frac{l^\mu}{D^3} = 0$, at the end it will be vanish so put here zero,

$$\begin{aligned} &= \bar{u}(p') [\not{l} \gamma^\mu \not{l}^\nu + 0 + (-y\not{q} + z\not{p}) \gamma^\mu \not{l} ((1-y)\not{q} + z\not{p})\\ &\quad + m^2 \gamma^\mu - 2m(q^\mu - 2yq^\mu + 2pz^\mu)] u(p), \quad (3.3.70)\\ &= \bar{u}(p') [\not{l} \gamma^\mu \not{l} + (-y\not{q} + z\not{p}) \gamma^\mu ((1-y)\not{q} + 2\not{p}) + m^2 \gamma^\mu\\ &\quad -2m(q^\mu - 2yq^\mu + 2zp^\mu] u(p), \quad (3.3.71) \end{aligned}$$

because of lengthy calculation we simplify very term of the of the upper equation individ-

ually, the first term is,

$$\begin{aligned} \not{l}\gamma^\mu\not{l} &= l_\alpha l_\beta \gamma^\alpha\gamma^\mu\gamma^\beta, = l_\alpha l_\beta \gamma^\alpha(2\eta^{\mu\beta} - \gamma^\beta\gamma^\mu), && (3.3.72)\\ &= l_\alpha l_\beta \left(\gamma^\alpha 2\eta^{\mu\beta} - \gamma^\alpha\gamma^\beta\gamma^\mu\right), = 2l_\alpha l^\mu\gamma^\alpha l^2 - l^2\gamma^\mu && (3.3.73)\\ &= 2\frac{1}{4}\eta^{\mu\nu}\gamma^\alpha l^2 - l^2\gamma^\mu, \text{ as } l^\mu l^\nu = \frac{1}{4}\eta^{\mu\nu}, = \frac{1}{2}l^2\gamma^\mu - l^2\gamma^\mu, = -\frac{1}{2}l^2\gamma^\mu && (3.3.74)\end{aligned}$$

Thus we have, numerator,

$$\begin{aligned} &= \bar{u}(p')\{-\frac{1}{2}\gamma^\mu l^2 + (-y\not{q} + z\not{p})\,\gamma^\mu\,((1-y)\not{q} + z\not{p}) && (3.3.75)\\ &\quad +m^2\gamma^\mu - 2m(q^\mu - 2yq^\mu + 2zp^\mu]u(p), \end{aligned}$$

lets take the second term of Eq. (3.3.75) and simplify it,

$$\begin{aligned} &\bar{u}(p')\left[(-yq' + z\not{p})\,\gamma^\mu\,((1-y)\not{q} + z\not{p})\right]u(p) && (3.3.76)\\ =\ &\bar{u}(p')\left[(-yq' + z\not{p})\,\gamma^\mu\,((1-y)\not{q} + mz)\right]u(p), && (3.3.77)\\ =\ &\bar{u}(p')\left((-y-z)\,\not{q} + mz\right)\gamma^\mu\left((1-y)\not{q} + mz\right)u(p), && (3.3.78)\\ =\ &\bar{u}(p')\left((x-1)\,\not{q} + mz\right)\gamma^\mu\left((1-y)\,\not{q} + mz\right)u(p), \text{ as x+y+z=1} && (3.3.79)\\ =\ &\bar{u}(p')\left((x-1)\,(1-y)\not{q}\gamma^\mu\not{q} + mz\,(x-1)\,\not{q}\gamma^\mu + mz\,(1-y)\,\gamma^\mu q + m^2z^2\gamma^\mu\right)u(p), \end{aligned}$$

$\not{q}\gamma^\mu\not{q} = \cancel{2q^\lambda\not{q}}^{\,0} - \gamma^\mu q^2$, so,

$$\begin{aligned} &\bar{u}(p')[(-yq' + z\not{p})\,\gamma^\mu\,((1-y)\not{q} + z\not{p})]u(p),\\ =\ &\bar{u}(p')[(x-1)\,(1-y)\left(-\gamma^\mu q^2\right) + mz\,(x-1)\,\not{q}\\ &\gamma^\mu + mz\,(1-y)\,\gamma^\mu q + m^2z^2\gamma^\mu]u(p). && (3.3.80)\end{aligned}$$

Now we are simplifying the second term of the upper Eq. (3.3.80),

$$\begin{aligned} \bar{u}(p')\,\not{q}\gamma^\mu u(p) &= \bar{u}(p')\,q\,\,(p' - \not{p})\,\gamma^\mu u(p), && (3.3.81)\\ &= \bar{u}(p')\,(m\gamma^\mu - \not{p}\gamma^\mu)\,u(p), && (3.3.82)\\ &= \bar{u}(p')\,\,(m\gamma^\mu - 2p^\mu + \gamma^\mu\not{p})\,\,u(p), \qquad \not{p}\gamma^\mu = 2p^\mu - \gamma^\mu\not{p} && (3.3.83)\\ &= \bar{u}(p')\,(2m\gamma^\mu - 2p^\mu)\,\,u(p), && (3.3.84)\end{aligned}$$

which implies,

$$\not{q}\gamma^\mu = 2m\gamma^\mu - 2p^\mu = 2\,(m\gamma^\mu - p^\mu)\,, \tag{3.3.85}$$

Eq. (3.3.80) follows,

$$\bar{u}(p')\left[(-yq' + z\not{p})\gamma^\mu\left((1-y)\not{q} + z\not{p}\right)\right]u(p) = \gamma^\mu\left((1-x)(1-y)q^2 + m^2z^2\right) + 2mz(1-y)q^\mu\gamma^\mu + (x+y-z)\not{q}\gamma^\mu,$$

so,

$$\bar{u}(p')\left[(-yq' + z\not{p})\gamma^\mu\left((1-y)\not{q} + z\not{p}\right)\right]u(p) \tag{3.3.86}$$

$$= \gamma^\mu\left((1-x)(1-y)q^2 + m^2z^2\right) + 2mz(1-y)q^\mu\gamma^\mu + (x+y-z)\not{q}\gamma^\mu, \tag{3.3.87}$$

$x + y + y = 1$. The second and third term of Eq. (3.3.75),

$$\bar{u}(p')\left\{(-y\not{q} + z\not{p})\gamma^\mu\left((1-y)\not{q} + z\not{p}\right) + m^2\gamma^\mu\right\}u(p), \tag{3.3.88}$$

$$= \bar{u}(p')\left[\gamma^\mu\left\{(1-x)(1-y)q^2 + m^2\left(-2z - z^2\right)\right\} + 2mz(1-y)q^\mu + 2mz(1+z)p^\mu\right]u(p),$$

The first two simplification in the numerator is,

$$\bar{u}(p')\left[-\frac{1}{2}\gamma^\mu l^2 + (-y\not{q} + z\not{p})\gamma^\mu\left((1-y)\not{q} + z\not{p}\right) + m^2\gamma^\mu - 2m\left(q^\mu - 2yq^\mu + 2zp^\mu\right)\right]u(p), \tag{3.3.89}$$

After combining the last two terms and performing a little bit of simplification, the expression has been modified

$$numerator = \bar{u}(p')[\gamma^\mu\left[-\frac{1}{2}l^2 + (1+x)(1-y))q^2 + \left(1 - 2z - z^2\right)m^2\right] + mz(z-1)(p'^\mu - p^\mu) + m(2-z)((y-x)q^\mu]u(p), \tag{3.3.90}$$

$\triangle = -xyq^2 + (1-z)^2m^2$, is even under the exchange of x and y, and when we perform integral at last, the last term in the upper expression become zero because $\int dxdy \frac{(x-y)}{\text{even funtion of (xy)}} = 0$, so,

$$numerator = \bar{u}(p'\left[\gamma^\mu\left\{-\frac{1}{2}l^2 + (1+x)(1-y)q^2 + \left(1 - 2z - z^2\right)m^2\right\} + mz(z-1)(p'^\mu - p^\mu)\right]u(p),$$

use garden identity $\bar{u}(q_2)\gamma^\mu u(q_1) = \bar{u}(q_2)\left\{\frac{p'^\mu - p^\mu}{2m} + \iota\frac{\sigma^{\mu\nu}q_\nu}{2m}\right\}u(q_1)$,

$$numerator = \bar{u}(p'[\gamma^\mu\left\{-\frac{1}{2}l^2 + (1+x)(1-y)q^2 + \left(1 - 2z - z^2\right)m^2\right\} + \frac{\iota\sigma^{\mu\nu}q_\nu}{2m}2mz(z-1)]u(p), \tag{3.3.91}$$

put the numerator in the following equation,

$$\begin{aligned}\bar{u}(p')\delta\,\Gamma^{\mu}u(p) &= 2\iota e^2\int\frac{dl^4}{(2\pi)^4}\int_0^1 dxdydz\delta(x+y+z-1)\frac{1}{D^3}\times\text{numerator}, \\ &= 2\iota e^2\int\frac{dl^4}{(2\pi)^4}\int_0^1 dxdydz\delta(x+y+z-1)\frac{1}{D^3} \\ &\quad\times\bar{u}(p'\left[\gamma^{\mu}\left\{-\frac{1}{2}l^2+(1+x)(1-y)q^2+\left(1-2z-z^2\right)m^2\right\}+\frac{\iota\sigma^{\mu\nu}q_{\nu}}{2m}2mz(z-1)\right],\end{aligned} \tag{3.3.92}$$

as $D=l^2+\triangle+i\epsilon$, where $\triangle=-xyq^2(1-z)^2m^2$,as $q^2<0$ implies $\triangle>0$.

wick rotation $l_0\to l_E=-il_0$, $l_E=(il_0,l_\iota)$

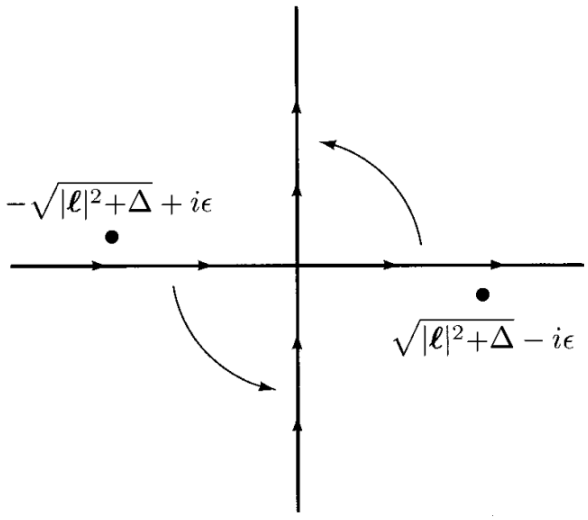

Figure 3.3.4: The contour of the l^0 integration can be rotated as shown [18].

$$\bar{u}(p')\delta\,\Gamma^{\mu}u(p) = 2ie^2\int\frac{dl^4}{(2\pi)^4}\int_0^1 dxdydz\int\frac{d^4l_E}{(4\pi)^4}(-----), \tag{3.3.93}$$

We need to evaluate integration of the kind $\int\frac{dl^4}{(2\pi)^4}\frac{1}{(l^2-\triangle)^m}$, and $\int\frac{dl^4}{(2\pi)^4}\frac{l^2}{(l^2-\triangle)^m}$, by performing wick rotation,

$$\int\frac{dl^4}{(2\pi)^4}\frac{1}{(l^2-\triangle)^m} = \frac{\iota}{(-1)^m}\frac{1}{(2\pi)^4}\int d^4l_E\frac{1}{(l_E^2+\triangle)^m}, \tag{3.3.94}$$

$d^4l_E = d\Omega_3 l^3 dl_E$,

$$\int \frac{dl^4}{(2\pi)^4}\frac{1}{(l^2-\triangle)^m} = \frac{i\,(-1)^m}{(2\pi)^4}\int d\Omega_3 \int_0^\infty dl_E \frac{l^3}{(l_E^2+\triangle)^m}, \tag{3.3.95}$$

$\int d\Omega_3$is unit sphere equal to $2\pi^2$,

$$\begin{aligned}\int \frac{dl^4}{(2\pi)^4}\frac{1}{(l^2-\triangle)^m} &= \frac{i\,(-1)}{(2\pi)^4}\left(2\pi^2\right)\int dl_E \frac{l^3}{(l_E^2+\triangle)^m}, \qquad (3.3.96)\\ &= \frac{i\,(-1)^m}{8\pi^2}\int l d_E l_E \frac{l_E^2}{(l_E^2+\triangle)^m}, = \frac{i\,(-1)^m}{8\pi^2}\int_0^\infty \frac{2}{2} l_E dl_E \frac{l_E^2}{(l_E^2+\triangle)^m},\end{aligned}$$

let $\alpha = l_E^2 + \triangle,\ \Longrightarrow\ d\alpha = 2l_E dl_E$,

$$\begin{aligned}\int \frac{dl^4}{(2\pi)^4}\frac{1}{(l^2-\triangle)^m} &= \frac{i\,(-1)^m}{2\,(2\pi)^4}\int_\triangle^\infty \frac{(\alpha-\triangle)}{\alpha^m}d\alpha, \qquad (3.3.97)\\ &= \frac{2i\,(-1)^m}{(2\pi)^4}\frac{1}{(m-1)\,(m-2)}\frac{1}{\triangle^{m-2}},\end{aligned}$$

and we can write the $\int \frac{dl^4}{(2\pi)^4}\frac{l^2}{(l^2-\triangle)^m}$ by performing wick rotation as,

$$\begin{aligned}\int \frac{dl^4}{(2\pi)^4}\frac{l^2}{((l^2-\triangle)} &= \frac{i(-1)^{m-1}}{(2\pi)^4}\int dl_E \frac{l_E^2}{(l_E^2+\triangle)^m}, \qquad (3.3.98)\\ &= \frac{i(-1)^{m-1}}{4\pi^2}\frac{2}{(m-1)\,(m-2)\,(m-3)}\frac{1}{\triangle^{m-3}}, \qquad (3.3.99)\end{aligned}$$

the upper equation divergent at $m = 3$.

We have two form factors, one $F_1(q^{2)}$*and*other one $F_2(q^2)$. it doesn't give contribution to $F(q_2^2)$ because $F(q^2)$ does not involve integration of $\int d^4l \frac{l^2}{(-----)}$type , so $F(q^2)$ is actually divergent we will introduce a perturb in p. so that the last integration gives us a finite answer. $\frac{1}{(k-p)^2+i\epsilon}$, in this photon propagator K take all the value from 0 to . we will keep up to some momentum k', and ignore photons of higher momentum. so,

$$\frac{1}{(k-p)+i\epsilon} \longrightarrow \left(\frac{1}{(k-p)+\iota\epsilon} - \frac{1}{(k-p)^2-\Lambda^2+i\epsilon}\right), \tag{3.3.100}$$

this implies that,

$$\int \frac{dl^4}{(2\pi)^4}\frac{1}{(l^2-\triangle)^m} = \int \frac{dl^4}{((2\pi)}\left(\frac{1}{(l^2-\triangle)^3} - \frac{1}{(l^2-\triangle_\Lambda)^3}\right), \tag{3.3.101}$$

where $\triangle_\Lambda = -xyq^2 + (1-z)^2 m^2 + z\triangle$,

$$\int \frac{dl^4}{(2\pi)^4} \frac{1}{(l^2 - \triangle)^m} = \frac{i}{(2\pi)^4} log\left(\frac{\triangle_\Lambda}{\triangle}\right) + \left(\Lambda^{-2}\right)\cdots . \tag{3.3.102}$$

The first term is the divergent term contribute to $F_1(q^2)$.

$$\delta F_1(q^2) \longrightarrow \delta F_1(q^2) - \delta F(0), \tag{3.3.103}$$

$F_1(0) = 1$, when the photon momentum goes to ∞ the integration goes to become divergent. Called ultraviolet divergent at low energy divergent also occur called infrared divergent,

$$\int_0^1 dxdydz \frac{1 - 4z + z^2}{\triangle(q^2 = 0)} \delta(x + y + z - 1), \tag{3.3.104}$$

$$= \int_0^1 dxdydz\delta(x + y + z - 1) \frac{1 - 4z + z^2}{m^2 (1 - z)^2}, \tag{3.3.105}$$

$$= \int_0^1 dz \int_0^{1-z} dy \left(\int_0^{1-z-y} dx\delta(x + y + z - 1)\right) \frac{1 - 4z - z^2}{m^2 (1 - z)^2}, \tag{3.3.106}$$

$$= \int_0^1 dz \int_0^{1-z} dy \frac{1 - 4z - z^2}{m^2 (1 - z)}, \tag{3.3.107}$$

$$= \int_0^1 dz \int_0^{1-z} dy \frac{-2 - (1 - z)(3 - z)}{m^2 (1 - z)^2}, \tag{3.3.108}$$

$$= \int_0^1 dz \int_0^{1-z} dy \left(\frac{-2}{m^2((1 - z)}\right) + \cdots\cdots , \tag{3.3.109}$$

because of $(1-z)^2$there is divergent all divergence appear in $F_1(q^2)$ term. Our are entrust in $F_2(q^2)$ correction to the anomalous magnetic moment of electron(any leptons) which is given by $F_2(q^2)$ term, the first order correction yo $F_2(q^2)$. let compute,

$$F_2(q^2) = \frac{\alpha}{2\pi} \int_0^1 dxdydz \frac{2m^2 z (1 - z)}{m^2 (1 - z)^2 - xyq^2}, \tag{3.3.110}$$

$$F_2(q^2 = 0) = \frac{\alpha}{2\pi} \int_0^1 dxdydz \frac{2m^2 z (1 - z)}{m^2 (1 - z)^2}, \tag{3.3.111}$$

$$F_2(0) = \frac{\alpha}{2\pi}\int_0^1 dx \int_0^1 dz \int_0^{1-z} dy \frac{2z}{(1-z)}, \tag{3.3.112}$$

$$= = \frac{\alpha}{2\pi}\int_0^1 2zdz = \frac{\alpha}{2\pi}\int_0^1 2zdz = \frac{\alpha}{2\pi}, \tag{3.3.113}$$

$$= \frac{\alpha}{2\pi} = \frac{g-2}{2} = 0..0011614, \tag{3.3.114}$$

$$F_2(0) = 0.0011614 \tag{3.3.115}$$

This outcome is referred to as the Schwinger term, which signifies the first order correction in QED and is significantly the most substantial radiative correction.

so,

$$g = 2\left(1+\frac{\alpha}{2\pi}\right) = 2\left(1+a_\mu\right) \tag{3.3.116}$$

$$a_\mu = 0.0011614, \tag{3.3.117}$$

This is only the first order correction [18].The higher order correction also contributed corresponding to the diagram given below.

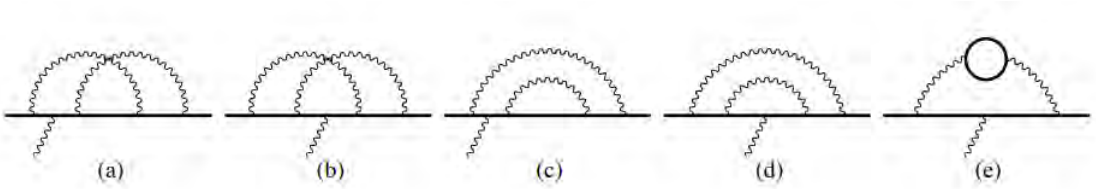

Figure 3.3.5: 4^{th} order vertex diagrams. There are a total of seven such diagrams, but the reverse-time versions of diagrams (a) and (c) are not depicted [19].

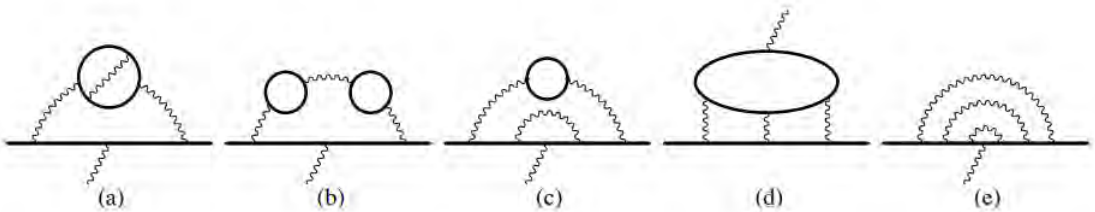

Figure 3.3.6: : 6^{th} order diagrams. total of 72 diagrams are present and they are categorized into five sets that are gauge-invariant. Examples from each set are represented as (a) to (e). [19].

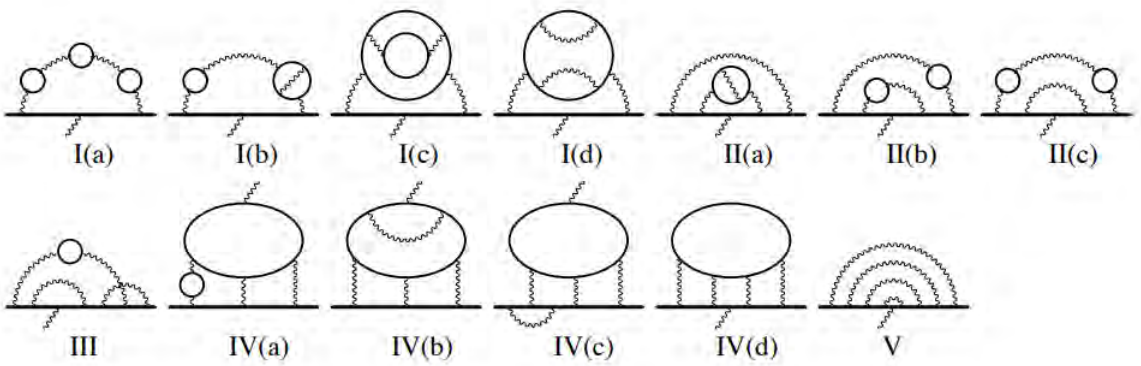

Figure 3.3.7: 8^{th} order diagrams. There are total 891 diagrams [19].

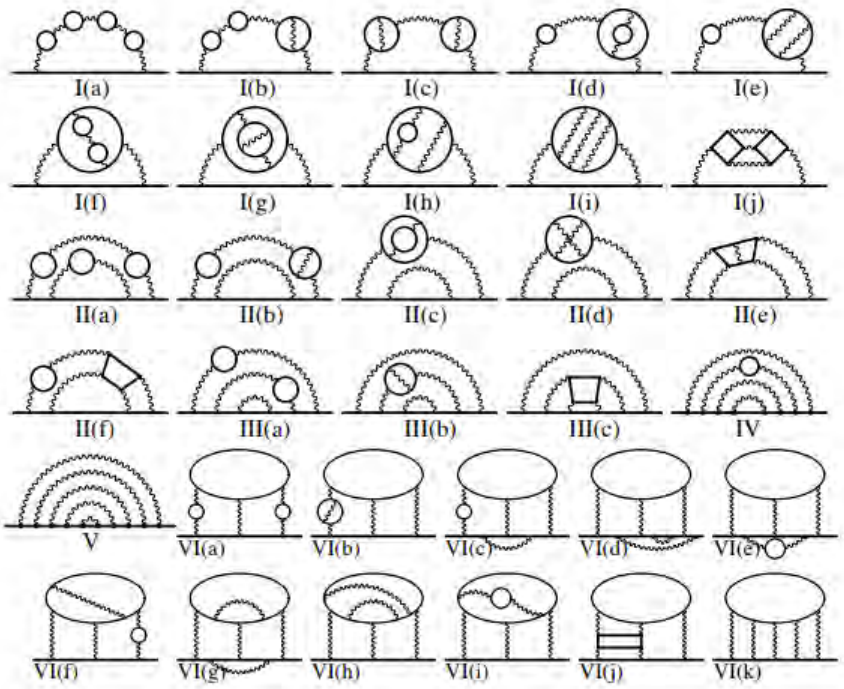

Figure 3.3.8: 10^{th} vertex diagrams. There are total 12672 diagrams [19].

Order	with α(Cs)	with $\alpha(a_e)$
2	116 140 973.321(23)	116 140 973.233(28)
4	413 217.6258(70)	413 217.6252(70)
6	30 141.90233(33)	30 141.90226(33)
8	381.004(17)	381.004(17)
10	5.0783(59)	5.0783(59)
a_μ(QED)	116 584 718.931(30)	116 584 718.842(34)

Figure 3.3.9: Contributions to $g_\mu - 2$ from QED units of 10^{-11} [19].

The total contribution from all possible QED diagrams is,

$$a_\mu^{QED} = 116584718.842(34) \times 10^{-11}. \tag{3.3.118}$$

3.3.2 Electroweak Contribution

All possible one loop contribution are shown in the Fig. 3.3.10.

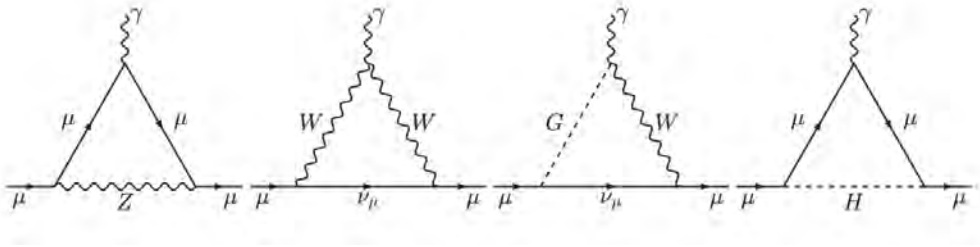

Figure 3.3.10: One-loop EW Feynman diagrams [19].

The masses bosons have a significant suppressive effect on the EW contributions to a_μ.The value for total a_μ^{EW} is given as [4][20][21],

$$a_\mu^{EW} = 153.6(1.0) \times 10^{-11}. \tag{3.3.119}$$

3.3.3 Hadronic Contribution

In general, data-driven methods can be used to determine the Hadronic vacuum polarization (HVP) contributions (shows in third diagram in Fig. 3.3.1). Using either data from

$e^+ + e^- \rightarrow$ hadrons measurements or information obtained from Lattice QCD as an input for dispersion relations.

3.3.4 Data-driven HVP

3.3.4.1 Data-driven Calculation a_μ^{HVP}

The contribution of the hadronic vacuum polarization to the muon magnetic moment can be estimated using the data on the hadronic cross-section (σ_{had}) and the optical theorem, at the leading order [4] [22],

$$a^{LOHVP} = \frac{1}{4\pi}\int_{4m_\pi^2}^{\infty} ds\, K(s)\sigma_{had}(s), \tag{3.3.120}$$

σ_{had} is the bare $e^+e^- \rightarrow \gamma* \rightarrow hadrons(\gamma)$ cross-section, and the kernel function reads,

$$K(s) = \frac{x^2}{2}\left(2-x^3\right) + \frac{1+x}{1-x}x^2 logx + \frac{\left(1+x^2\right)\left(1+x\right)^2}{x^2}\left(log(1+x) - x + \frac{x^2}{2}\right),$$

where $x = (1-\beta_\mu)/(1+\beta)_\mu$and $\beta_\mu = (1-4m_\mu^2/s)^{1/2}$. The $g_\mu - 2$ Theory Initiative has suggested the numerical value based on the analyses in Refs [23][24][25],

$$a_\mu^{LO,HVP} = 693.1 \pm 4.0 \times 10^{-10}. \tag{3.3.121}$$

There are several data-driven evaluations of a_μ^{HVP} that vary in their handling of the data and the functional forms of the cross section assumptions made. The DHMZ [26] and KNT [27] groups utilize the raw cross section directly, while the CHHKS group utilizes a different approach by evaluating the contributions from the $\pi^0\gamma$, 2π, and 3π channels with additional restrictions from analyticity and unitarity [28]. The results from these groups have been combined to account for differences among the groups and tensions between data sets. This results in $a_\mu^{LOHVP} = 6931(40) \times 10^{-11}$ [4], $a_\mu^{NLOHVP} = -98.3(7) \times 10^{-11}$[24], and $a_\mu^{NLOHVP} = 12.4(1) \times 10^{-11}$ [29], yielding the total HVP contribution of [4],

$$a_\mu^{HVP} = 6845\,(40) \times 10^{-11}. \tag{3.3.122}$$

3.3.4.2 HVP from Lattice QCD

The findings of the distinct flavor contributions from different lattice groups and the overall estimation of a_μ^{LOHVP} are illustrated in Figure 3.3.11. A conservative method is used to combined the results from the $ETM18/19$ [30], [31] $Mainz/CLS-19$ [32],

$FHM-19$ [33] ,[34], $PACS-19$ [35], $RBC/UKQCD-18$ [36], and $BMW-17$ [37] into an average obtained from the lattice results in reference [36], with a value of $a_\mu^{LOHVP} = 711.6(18.4) \times 10^{-10}$blue band show in Fig. 3.3.11. The range between the data-driven approaches and the no-NP scenario is represented by the green band on these results. However, the errors are typically too big to draw any firm conclusions. Recently, the results of two analyses, $LM-20$ and $BMW-20$, found the values of a_μ^{LOHVP} to be $714(30) \times 10^{-10}$ [36] and $707.5(5.5) \times 10^{-10}$ respectively [37]. The latter is the first sub-percent precision lattice result for a_μ^{LOHVP}. It is below 1.3σ from the no-NP scenario and higher then 2.1σ from data-driven result.

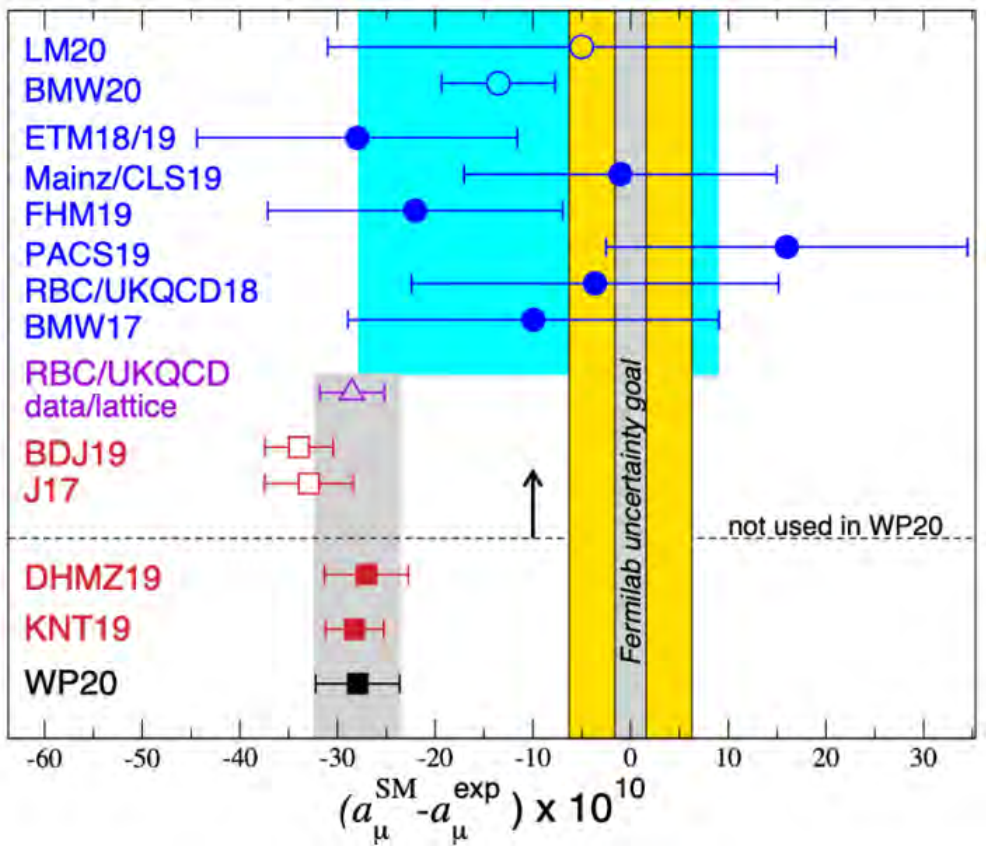

Figure 3.3.11: The yellow band signifies a scenario with no new physics. The red squares represent the results obtained from data-driven calculations of a_μ^{LOHVP}. The grey band in the middle represents the estimated uncertainty from the Fermilab $g_\mu - 2$ experiment. The dark blue filled circles show the results from lattice calculations, which are represented by the light-blue band [2].

3.3.5 Data-driven and Dispersive HLbL

There have been many important advancements in the calculations of sub-leading contributions in a model-dependent manner using up-to-date data-driven and dispersive methods to find a_μ^{HLbL} [39, 40, 41, 42]. Whenever feasible, hadronic insertions utilize experimental data as input, but if not available, theoretical calculations of amplitudes are utilized as an alternative. The HLbL tensor can be expressed as the sum of all intermediate states, both direct and crossed, such as. $\Pi_{\mu\nu\lambda\sigma} = \Pi_{\mu\nu\lambda\sigma}^{\pi^0-pole} + \Pi_{\mu\nu\lambda\sigma}^{\pi-box} + \Pi_{\mu\nu\lambda\sigma}^{\pi\pi} + ...$ As a result,

$$a_\mu^{HLbL} = a_\mu^{\pi^0-pole} + a_\mu^{\pi-box} + a_\mu^{\pi\pi} + ... \tag{3.3.123}$$

The numbers from the various contributions are added up to create a data-driven, dispersive estimate for the total a_μ^{HLbL} is,

$$a_\mu^{HLbL} = 92\,(19) \times 10^{-11}. \tag{3.3.124}$$

The result of the NLO HLbL contribution is $a^{NLOHLbL} = 2(1) \times 10^{-11}$[4].

3.4 Comparing Experimental and Theoretical Results

The Brokheven $E821$ result is [43],

$$a_\mu^{BNL} = 116592091\,(63) \times 10^{-11}. \tag{3.4.1}$$

The combined result of Fermilab and BNL is [44],

$$a_\mu^{Exp} = a_\mu^{BNL+FNAL} = 116592061\,(41) \times 10^{-11}, \tag{3.4.2}$$

The SM contribution,

$$a_\mu^{QED} = 116584718.9\,(1) \times 10^{-11}, \tag{3.4.3}$$

$$a_\mu^{EW} = 153.6\,(1) \times 10^{-11}, \tag{3.4.4}$$

$$a^{HVP,LO} = 6931\,(40) \times 10^{-11}, \tag{3.4.5}$$

$$a_\mu^{HVP,NNLO} = 12.4\,(1) \times 10^{-11}, \tag{3.4.6}$$

$$a_\mu^{HLBL} + a_\mu^{HLBL,NLO} = 92\,(18) \times 10^{-11}, \tag{3.4.7}$$

The total SM contribution is,

$$a_\mu^{SM} = 116591810\,(43) \times 10^{-11}, \tag{3.4.8}$$

Where the hadronic contributions in HVP and HLBL are the predominant sources of uncertainty. The deviation experimental and SM is,

$$a_\mu^{Exp} - a_\mu^{SM} = 251\,(59) \times 10^{-11}. \tag{3.4.9}$$

which is 4.2σ. As an alternative, a first-principle lattice QCD method has been used to calculate the HVP contribution [4][45]. Recently, the BMWc calculated the dominant HVP contribution to the $g_\mu - 2$ with high precision, achieving sub-percent accuracy, yielding a value, $(a_\mu^{HVP})^{BMW}$, which is larger than $(a_\mu^{HVP})^{TI}_{e^+e^-}$ [46]. If we had utilized $(a_\mu^{HVP})^{BMW}$ instead of $(a_\mu^{HVP})^{TI}_{e^+e^-}$, the difference with a_μ^{Exp} would have been reduced to 1.6 standard deviation. The outcome would be accordingly,

$$\left(a_\mu^{HVP}\right)^{TI}_{e^+e^-} = 6931\,(40) \times 10^{-11}. \tag{3.4.10}$$

$$\left(a_\mu^{HVP}\right)^{BMW} = 7075\,(50) \times 10^{-11}. \tag{3.4.11}$$

1.6σ discrepancy means there is no NP. We called difference between $(a_\mu^{HVP})^{BMW}$ and $(a_\mu^{HVP})^{TI}_{e^+e^-}$ as the new $g_\mu - 2$ puzzle, and our work of next chapter is to solve this new puzzle.

Chapter 4

Solution of the New Muon $g-2$ Puzzle

Here we are going to study how to solve the new muon $g-2$ puzzle, when $(a_\mu^{HVP})^{TI}_{e^+e^-}$ and $(a_\mu^{HVP})^{BMW}$ are assume to be correct, then we can ask what is missing due to which these both are differ by 2.1σ from each other, thanks to NP effects, the discrepancy between $(a_\mu^{HVP})^{TI}_{e^+e^-}$ and $(a_\mu^{HVP})^{BMW}$ is expected to be resolved without disrupting the existing 1.6σ discrepancy between $(a_\mu^{HVP})^{BMW}$ and $(a_\mu^{HVP})^{EXP}$. We don't consider a direct NP contribution to Δa_μin this case. In reality, this may only resolve the old $g_\mu - 2$ puzzle , not the new one. To address the new $g_\mu - 2$ puzzle, it is necessary to consider NP that modifies the $e^+e^- \to \sigma_{had}$.

A suggestion has already been made to raise σ_{had} due to an unforeseen missing contribution , in order to improve $(a_\mu^{HVP})^{TI}_{e^+e^-}$ and resolve Δa_μ [47, 48, 49, 50, 51]. However, the required shift in σ_{had} is is not supported by the electroweak fit if $\sqrt{s} \lesssim 1GeV$ [49]. Therefore, NP modification of $\sigma_{had'}$ will be consider below the GeV scale. While the origin of the shift in σ_{had} was not specified in [47, 48, 49, 50, 51] . Here we assumed that it was caused by NP. For the first time, we examine the significant impact of NP on the results of e^+e^- and BMWc lattice after categorizing its general characteristics in a model-independent way.

The dispersion relation is crucial for our analysis to determine $(a_\mu^{HVP})^{TI}_{e^+e^-}$ through σ_{had}. It will be shown that new $g_\mu - 2$ puzzle cannot be solved in situations where NP only couples to hadrons. In this case, the value that should be used in the dispersion relation to calculate the HVP contribution is not the experimental σ_{had}, but rather $\sigma_{had} - \Delta\sigma^{NP}_{had}$. Therefore, by causing negative interference between NP and SM, the discrepancy between $(a_\mu^{HVP})^{TI}_{e^+e^-}$and $(a_\mu^{HVP})^{BMW}$ might be resolved, that is $\Delta\sigma^{NP}_{had} < 0$. As we will show later, the picture shown selects a specific scenario for NP that requires light particles with a

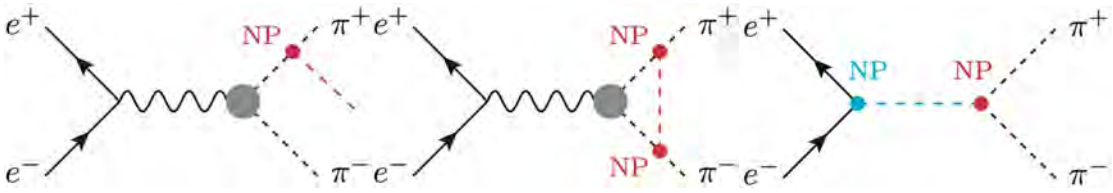

Figure 4.0.1: possibilities of NP contributions to σ_{had} through FSR (1^{st} and 2^{nd} diagrams) and through a NP tree-level intermediary that is connected to both hadrons and electrons (3^{rd} diagram).

mass around or less than 1 GeV to interact with SM fermions through a vector current.

Model-independent Analysis

Here we solve the new $g_\mu - 2$ puzzle through NP models for this we modify σ_{had}. With this objective in mind, we present the concept of the dispersion relation,

$$(a_\mu^{HVP})_{e^+e^-} = \frac{\alpha}{\pi^2}\int_{m_\pi^2}^{\infty}\frac{ds}{s}K(s)Im\Pi_{had}(s), \tag{4.0.1}$$

where $K(s)$ is the kernel function, for $\sqrt{s} \gg m_\mu$, $K(s) \approx m_\mu^2/3s$. Photon HVP, Π_{had}, includes NP effects Eq. (4.0.1). If NP does not interact with electrons and is not included in the σ_{had} at the tree-level, Eq. (4.0.1) can be expressed as,

$$(a_\mu^{HVP})_{e^+e^-} = \frac{1}{4\pi^3}\int_{m_{\pi^0}^2}^{\infty} dsK(s)\sigma_{had}(s), \tag{4.0.2}$$

where the impact of vacuum polarization and initial-state radiation is removed, but the hadronic cross section includes final-state radiation (FSR). Our focus will be on the region where the hadronic cross section is experimentally established, i.e. where $\sqrt{s}$ is greater than 0.3 GeV. This region makes a larger contribution to the integral in Eq. (4.0.2).

We display in Fig. 4.0.1 how NP can enter σ_{had}. The FSR , first and second diagram in Fig. 4.0.1 also effects the photon HVP at NLO The NP contaminations in ISR (Initial State Radiation) are ignored due to the strong limits on the NP coupling to electrons.

Restriction on NP couple to electron are quite strict therefor we ignore NP contaminations in ISR. In last diagram in Fig. 4.0.1 NP enter the σ_{had} coupling to electrons and hadrons at tree-level, at NLO photon HVP is also modifies due to the NP. However, it is crucial to note that its main contribution to $g_\mu - 2$ emerges through tree-level shift of σ_{had}. Therefore, there are two possibilities whether NP couple to both electrons and hadrons or to electrons alone. We examine these possibilities and there potential to resole the new $g_\mu - 2$ puzzle.

1. NP Coupled to Hadron Only

The first and second diagrams of Fig. 4.0.1 represent this scenario. Since the scalar QED estimate for the full photon FSR effect is only 50×10^{-11} [4] [53], well below the difference between E.q (3.4.10) and E.q (3.4.11), in addition the fact that SM particles couplings with NP are tightly constrained, in FSR new $g_\mu - 2$ puzzle cannot solve through NP contributions.

2. NP Coupled Both to Electrons and Hadrons

Only subtracted cross-section $\sigma_{had} - \Delta\sigma_{had}^{NP}$ should be include in Eq. (4.0.2) If NP contributes to hadronic cross-section at the tree-level (last diagram in Fig. 4.0.1). We point out that if $\Delta\sigma_{had}^{NP} < 0$, the latter can be larger than σ_{had}, requiring that that negative interference with the SM is the main factor that causes the NP effect to be substantial. Using σ_{had} , $(a_\mu^{HVP})_{e^+e^-}^{TI}$ has been calculated rather rather than $\sigma_{had} - \Delta\sigma_{had}^{NP}$, the theoretical prediction of a_μ^{HVP} Eq. (4.0.2) is,

$$\left(a_\mu^{HVP}\right)_{e^+e^-} \;=\; \left(a_\mu^{HVP}\right)_{e^+e^-}^{TI} + \left(a_\mu^{HVP}\right)_{NP}. \tag{4.0.3}$$

$(a_\mu^{HVP})^{NP}$ describes NP effects at LO and NLO as a result of the NP mediator's tree-level exchange see last in Fig.4.0.1 . Instead, only NLO NP effects should cause $(a_\mu^{HVP})^{BMW}$ to shift. Surprisingly, this scenario might make it possible to match Eq. (4.0.3) with $(a_\mu^{HVP})_{EXP}$ while maintaining agreement with the BMWc conclusion.

Light New Physics Analysis

We are looking into the possibility of accurately and effectively representing the second scenario discussed earlier in a clear NP model. Due to the scaling of $K(s)$ to $1/s$ and the fact that changes to hadronic cross-section above 1 GeV are not supported by electroweak precision tests [49], we are focusing on the energy region below 1 GeV, where the $e^+e^- \to \pi^+\pi^-$ channel makes up the majority of the contribution to hadronic cross-section. This channel contributes more than 70% to the $g_\mu - 2$ value in the SM, which is generated by hadrons. Scalar couplings interference with the SM vector current is suppressed by the mass of electron, while pseudo-scalar and axial couplings are not. With this in mind, our focus is on the exchange of Z' "light boson", which has vector interactions with both electrons and first-generation quarks, at the tree-level,

$$L_{Z'} \supset \left(g_V^e \bar{e}\gamma^\mu e + g_V^q \bar{q}\gamma^\mu q\right) Z'_\mu, \tag{4.0.4}$$

where $m_{z'} \lesssim 1GeV$ and $q = u, d$. The vector form factor of pion can serve as a representation of the matrix element associated with the intermediate state involving two pions,

$$< \pi^{\pm}(p')|J^{\mu}_{em}(0)|\pi^{\pm}(p) >= \pm (p' + p)^{\mu} F^{V}_{\pi}(q^2 = (p' - p)^2). \tag{4.0.5}$$

where $J^{\mu}_{em} = \frac{2}{3}\bar{u}\gamma^{\mu}u - \frac{1}{3}\bar{d}\gamma^{\mu}d$ is the electromagnetic current. In the limit where ISO-spin symmetry is present, by taking use of the charge conjugation in-variance, we find,

$$< \pi^{\mp}|J^{\mu}_{em}|\pi^{\pm} >= - < \pi^{\pm}|\bar{d}\,\gamma^{\mu}\,d|\pi^{\mp} >=< \pi^{\mp}|\bar{u}\,\gamma^{\mu}\,u|\pi^{\pm} >, \tag{4.0.6}$$

Consequently, the Z' quark current's matrix element, $J^{\mu}_{Z'} = g^{u}_{V}\bar{u}\gamma^{\mu}u + g^{d}_{V}\bar{d}\gamma^{\mu}d$,

$$< \pi^{\pm}(p\prime)|J^{\mu}_{Z\prime}(0)|\pi^{\mp}(p) >= \pm(p\prime + p)^{\mu} \times F^{V}_{\pi}(q^2) \times (g^{u}_{V} - g^{d}_{V}), \tag{4.0.7}$$

contribution to the $\pi^{+}\pi^{-}$ amplitude vanishes if the Z' interactions in the limit where ISO-spin symmetry is present , as shown by the equations $g^{u}_{V} = g^{d}_{V}$.

The amplitude when $e^{-}e^{+} \to \pi^{-}\pi^{+}$ through SM particle photon is,

$$M^{SM} \;=\; -\iota e^2 \bar{u}\gamma^{\mu}u\frac{1}{q^2} \cdot \pm (p' + p)^{\mu} F^{V}_{\pi}(q^2). \tag{4.0.8}$$

And the amplitude of the interaction $e^{-}e^{+} \to \pi^{-}\pi^{+}$ through Z' NP,

$$M^{NP} \;=\; -\iota g^{e}_{V}\bar{u}\gamma^{\mu}u\frac{1}{q^2 - m^2_{Z'} + im_{Z'}\Gamma_{Z'}} \cdot \pm (p' + p)^{\mu} F^{V}_{\pi}(q^2)\left(g^{u}_{V} - g^{d}_{V}\right). \tag{4.0.9}$$

The combined amplitude,

$$\begin{aligned} M^{SM+NP} &= M^{SM} + M^{NP}, && (4.0.10)\\ &= -ie^2\bar{u}\gamma^{\mu}u\frac{1}{q^2} \cdot \pm (p' + p)^{\mu} F^{V}_{\pi}(q^2) - ig^{e}_{V}\bar{u}\gamma^{\mu}u\frac{1}{q^2 - m^2_{Z'} + im_{Z'}\Gamma_{Z'}} \times \\ &\quad \pm (p' + p)^{\mu} F^{V}_{\pi}(q^2)\left(g^{u}_{V} - g^{d}_{V}\right), && (4.0.11)\\ &= -i\bar{u}\gamma^{\mu}u \cdot \pm (p' + p)^{\mu} F^{V}_{\pi}(q^2)\left\{\frac{e^2}{q^2} + \frac{g^{e}_{V}\left(g^{u}_{V} - g^{d}_{V}\right)}{q^2 - m^2_{Z'} + im_{Z'}\Gamma_{Z'}}\right\}, && (4.0.12) \end{aligned}$$

lets define $K \equiv -\iota\bar{u}\gamma^{\mu}u \cdot \pm (p' + p)^{\mu} F^{V}_{\pi}(q^2)$ then,

$$M^{SM+Np} \;=\; K\left\{\frac{e^2}{q^2} + \frac{g^{e}_{V}\left(g^{u}_{V} - g^{d}_{V}\right)}{q^2 - m^2_{Z'} + im_{Z'}\Gamma_{Z'}}\right\}. \tag{4.0.13}$$

and Eq. (4.0.8) $\implies$ $M^{SM} = K\frac{e^2}{q^2}$, as cross-section σ is proportional to $|M|^2$,

$$\sigma^{SM} = K^2 \left|\frac{e^2}{q^2}\right|^2, \tag{4.0.14}$$

defining $\sigma^{SM+NP} = \sigma^{SM}_{\pi\pi} + \triangle\sigma^{NP}_{\pi\pi}$, is also proportional to the total amplitude square,

$$\sigma^{SM+NP} = \left|M^{SM+NP}\right|^2, \tag{4.0.15}$$

$$\sigma^{SM+NP} = K^2 \left|\frac{e^2}{q^2} + \frac{g^e_V\left(g^u_V - g^d_V\right)}{q^2 - m^2_{Z'} + im_{Z'}\Gamma_{Z'}}\right|^2, \tag{4.0.16}$$

$$\frac{\sigma^{SM+NP}}{\sigma^{SM}} = \frac{K^2}{K^2}\left|\frac{\frac{e^2}{q^2} + \frac{g^e_V\left(g^u_V - g^d_V\right)}{q^2 - m^2_{Z'} + im_{Z'}\Gamma_{Z'}}}{\frac{e^2}{q^2}}\right|^2, \tag{4.0.17}$$

$$\frac{\sigma^{SM+NP}}{\sigma^{SM}} = \left|1 + \frac{g^e_V\left(g^u_V - g^d_V\right)}{e^2}\frac{q^2}{q^2 - m^2_{Z'} + im_{Z'}\Gamma_{Z'}}\right|^2, \tag{4.0.18}$$

$$\frac{\sigma^{SM+NP}}{\sigma^{SM}} = \left|1 + \frac{g^e_V\left(g^u_V - g^d_V\right)}{e^2}\frac{s}{s - m^2_{Z'} + im_{Z'}\Gamma_{Z'}}\right|^2, \quad \text{as } q^2 = s, \tag{4.0.19}$$

The expression $\sigma_{had} - \triangle\sigma^{NP}_{had}$ can be utilized to determine $g_\mu - 2$ from both the SM and NP as described in Eq. (4.0.2). If it is assumed that the discrepancy in the hadronic cross-section, represented by Δa_μ, is resolved by NP, the result would be,

$$\triangle a_\mu = \frac{1}{4\pi^3}\int_{s_{exp}}^{\infty} dsK(s)\left(-\triangle\sigma^{NP}_{had}(0)\right), \tag{4.0.20}$$

where $s_{exp} \approx (0.3GeV)^2$, that is, for the $\pi\pi$ channel, the integration is performed within the data-driven region.

Now we are going to calculate $\triangle\sigma^{NP}_{had}$ from Eq. (4.0.19),

$$\frac{\sigma^{SM+NP}_{\pi\pi}}{\sigma^{SM}_{\pi\pi}} = \left|1 + \frac{g^e_V\left(g^u_V - g^d_V\right)}{e^2}\frac{s}{s - m^2_{Z'} + im_{Z'}\Gamma_{Z'}}\right|^2, \tag{4.0.21}$$

let define and introduce the effective coupling constant ϵ,

$$\epsilon \equiv \frac{g^e_V\left(g^u_V - g^d_V\right)}{e^2}, \quad and \;\; T \equiv \frac{s}{s - m^2_{Z'} + im_{Z'}\Gamma_{Z'}}, \tag{4.0.22}$$

$$\frac{\sigma_{\pi\pi}^{SM+NP}}{\sigma_{\pi\pi}^{SM}} = |1+\epsilon T|^2 = (1)^2 + (\epsilon T)^2 + 2\epsilon T, = 1 + \epsilon^2 T^2 + 2\epsilon T, \tag{4.0.23}$$

put the value of T,

$$\begin{aligned}
\frac{\sigma_{\pi\pi}^{SM+NP}}{\sigma_{\pi\pi}^{SM}} &= 1 + \epsilon^2 \frac{s^2}{\left(s - m_{Z'}^2 + i m_{Z'} \Gamma_{Z'}\right)^2} + \frac{2\epsilon s}{s - m_{Z'}^2 + i m_{Z'} \Gamma_{Z'}}, & (4.0.24)\\
\frac{\sigma_{\pi\pi}^{SM+NP}}{\sigma_{\pi\pi}^{SM}} &= 1 + \frac{\epsilon^2 s^2 + 2\epsilon s \left(s - m_{Z'}^2 + i m_{Z'} \Gamma_{Z'}\right)}{\left(s - m_{Z'}^2 + i m_{Z'} \Gamma_{Z'}\right)}, & (4.0.25)\\
\frac{\sigma_{\pi\pi}^{SM} + \triangle\sigma_{\pi\pi}^{NP}}{\sigma_{\pi\pi}^{SM}} &= 1 + \frac{\epsilon^2 s^2 + 2\epsilon s \left(s - m_{Z'}^2 + i m_{Z'} \Gamma_{Z'}\right)}{\left(s - m_{Z'}^2 + i m_{Z'} \Gamma_{Z'}\right)^2}, & (4.0.26)\\
\frac{\sigma_{\pi\pi}^{SM}}{\sigma_{\pi\pi}^{SM}} + \frac{\triangle\sigma_{\pi\pi}^{NP}}{\sigma_{\pi\pi}^{SM}} &= 1 + \frac{\epsilon^2 s^2 + 2\epsilon s \left(s - m_{Z'}^2 + i m_{Z'} \Gamma_{Z'}\right)}{\left(s - m_{Z'}^2 + i m_{Z'} \Gamma_{Z'}\right)^2}, & (4.0.27)\\
1 + \frac{\triangle\sigma_{\pi\pi}^{NP}}{\sigma_{\pi\pi}^{SM}} &= 1 + \frac{\epsilon^2 s^2 + 2\epsilon s \left(s - m_{Z'}^2 + i m_{Z'} \Gamma_{Z'}\right)}{\left(s - m_{Z'}^2 + i m_{Z'} \Gamma_{Z'}\right)^2}, & (4.0.28)\\
\frac{\triangle\sigma_{\pi\pi}^{NP}}{\sigma_{\pi\pi}^{SM}} &= \frac{\epsilon^2 s^2 + 2\epsilon s \left(s - m_{Z'}^2 + i m_{Z'} \Gamma_{Z'}\right)}{\left(s - m_{Z'}^2 + i m_{Z'} \Gamma_{Z'}\right)^2}, & (4.0.29)
\end{aligned}$$

approximating $\triangle\sigma_{had}^{NP} \approx \triangle\sigma_{\pi\pi}^{NP}$ we find,

$$\triangle\sigma_{had}^{NP}(s) \approx \sigma_{\pi\pi}^{SM}(s) \times \frac{2\epsilon s \left(s - m_{Z'}\right) + \epsilon^2 s^2}{\left(s - m_{Z'}^2\right)^2 + m_{Z'}^4 \gamma^2}, \tag{4.0.30}$$

where we introduce the parameter $\gamma \equiv \Gamma_{Z'}/m_{Z'}$. If channels ($Z' \longrightarrow e^+e^-$ and $Z' \longrightarrow \pi^+\pi^-$) both are kinematically allowed, then we want to fined $\gamma_{ee} = \frac{\Gamma_{Z'\to ee}}{m_{Z'}}$ and $\gamma_{\pi\pi} = \frac{\Gamma_{Z'\to\pi\pi}}{m_{Z'}}$.

$$\gamma_{ee} \approx \frac{\left(g_V^e\right)^2}{12\pi} = 2.7 \times 10^{-10} \left(\frac{g_V^e}{10^{-4}}\right)^2, \tag{4.0.31}$$

up to $(m_e/m_{Z^0})^4$corrections,

Now we are to going find $\gamma_{\pi\pi}$, as we know decay rate formula is given by,

$$\Gamma = \frac{S\,|P|}{8\pi m_{Z'}} |M|^2, \tag{4.0.32}$$

where S is the statistical factor that correct for double counting for example if $a \to b + b + b + c + c$ $S = \frac{1}{3!}\frac{1}{2!} = \frac{1}{12}$, and P is the magnitude of either outgoing momentum,

but here S=1 (no identical particle). The amplitude of the decay is,

$$M = < \pi^{\pm}(p\prime)|J^{\mu}_{Z'}(0)|\pi^{\mp}(p) > \varepsilon^{\mu}, \tag{4.0.33}$$

$$M = \pm (p' + p)^{\mu} F^{V}_{\pi}(q^2) \left(g^{u}_{V} - g^{d}_{V}\right) \epsilon^{\mu}, \tag{4.0.34}$$

$$|M|^2 = \left|\pm (p' + p)^{\mu} F^{V}_{\pi}(q^2) \left(g^{u}_{V} - g^{d}_{V}\right) \epsilon^{\mu}\right|^2, \tag{4.0.35}$$

$$|M|^2 = \left(g^{u}_{V} - g^{d}_{V}\right)^2 \left|F^{V}_{\pi}(q^2)\right|^2 (p' + p)^{\mu} (p' + p)^{\nu} \epsilon^{\mu}\epsilon^{\nu}, \tag{4.0.36}$$

$$|M|^2 = \left(g^{u}_{V} - g^{d}_{V}\right)^2 \left|F^{V}_{\pi}(q^2)\right| (p' + p)^{\mu} (p' + p)^{\nu} \frac{1}{3}\delta_{ij}, \tag{4.0.37}$$

$$|M|^2 = \frac{1}{3}\left(g^{u}_{V} - g^{d}_{V}\right)^2 \left|F^{V}_{\pi}(q^2)\right|^2 (p' + p)^{\mu} (p' + p)^{\nu} \delta_{ij}, \tag{4.0.38}$$

$$(p' + p)^{\mu} (p' + p)^{\nu} \delta_{ij} = 4P^2, \tag{4.0.39}$$

$$|M|^2 = \frac{1}{3}\left(g^{u}_{V} - g^{d}_{V}\right)^2 \left|F^{V}_{\pi}(q^2)\right|^2 4P^2, \tag{4.0.40}$$

$$|M|^2 = \frac{4}{3}\left(g^{u}_{V} - g^{d}_{V}\right)^2 \left|F^{V}_{\pi}(q^2)\right|^2 P^2, \tag{4.0.41}$$

put Eq. (4.0.41) in Eq. (4.0.32),

$$\Gamma = \frac{|P|}{8\pi m_{Z'}} \frac{4}{3}\left(g^{u}_{V} - g^{d}_{V}\right)^2 \left|F^{V}_{\pi}(q^2)\right|^2 P^2, \tag{4.0.42}$$

As $P = \frac{1}{2m_{Z'}}\sqrt{[m^2_{Z'} - (m_{\pi^+} + m_{\pi^-})^2][m^2_{Z'} - (m_{\pi^+} - m_{\pi^-})^2]}$ but $m_{\pi^+} = m_{\pi^-}$implies,

$$P = \frac{1}{2m_{Z'}}\sqrt{\left[m^2_{Z'} - (2m_{\pi})^2\right]\left[m^2_{Z'}\right]} = \frac{1}{2m_{Z'}}\sqrt{m^4_{Z'} - 4m^2_{\pi}m^2_{Z'}}, \tag{4.0.43}$$

$$= \frac{m^2_{Z'}}{2m_{Z'}}\sqrt{1 - \frac{4m^2_{\pi}}{m^2_{z'}}} = \frac{m_{Z'}}{2}\sqrt{1 - \frac{4m^2_{\pi}}{m^2_{z'}}} \tag{4.0.44}$$

put Eq. (4.0.44) in Eq. (4.0.42),

$$\Gamma = \frac{1}{8\pi m_{Z'}}\frac{4}{3}(g_V^u - g_V^d)^2 \left|F_\pi^V(q^2)\right|^2 \frac{m_{Z'}}{2}\sqrt{1-\frac{4m_\pi^2}{m_{z'}^2}}\left(\frac{m_{Z'}}{2}\sqrt{1-\frac{4m_\pi^2}{m_{z'}^2}}\right)^2, \quad (4.0.45)$$

$$\Gamma = \frac{1}{8\pi m_{Z'}}\frac{4}{3}(g_V^u - g_V^d)^2 \left|F_\pi^V(q^2)\right|^2 \frac{m_{Z'}^2}{2\times 4}\sqrt{1-\frac{4m_\pi^2}{m_{z'}^2}}\left(\sqrt{1-\frac{4m_\pi^2}{m_{z'}^2}}\right)^2, \quad (4.0.46)$$

$$\Gamma = \frac{1}{8\pi m_{Z'}}\frac{4}{3}(g_V^u - g_V^d)^2 \left|F_\pi^V(q^2)\right|^2 \frac{m_{Z'}^2}{2\times 4}\left(\sqrt{1-\frac{4m_\pi^2}{m_{z'}^2}}\right)^{2+1}, \quad (4.0.47)$$

$$\Gamma = \frac{(g_V^u - g_V^d)^2 m_{Z'}}{48\pi}|F_\pi^V(m_{Z^0}^2)|^2\left(1-\frac{4m_\pi^2}{m_{z'}^2}\right)^{3/2}, \quad (4.0.48)$$

as $\gamma_{\pi\pi} = \frac{\Gamma_{Z\to\pi\pi'}}{m_{Z'}}$ so,

$$\gamma_{\pi\pi} = \frac{(g_V^u - g_V^d)^2}{48\pi}|F_\pi^V(m_{Z^0}^2)|^2\left(1-\frac{4m_\pi^2}{m_{z'}^2}\right)^{3/2}. \quad (4.0.49)$$

ρ resonance can enhanced $|F_\pi^V(m_{Z^0}^2)|^2$ (normalized to $F_\pi^V(0)=1$) up to a factor of 45 [52]. For $m_{Z^0} < 2m_{\pi^+} \approx 0.28$GeV $\gamma = \gamma_{ee}$, for $m_{Z'} \in [0.3, 1]$ GeV , $\gamma \approx \gamma_{\pi\pi}$. As the tight bounds on g_V^e allow for the safely neglecting of the e^+e^- channel. The note states that if γ receives contributions from non-standard model final states, like decays into a dark sector, it will result in a definite positive change in σ_{had} since these contributions do not interfere with the SM. As a result, there will be a negative change in Δa_μ, worsening the discrepancy as indicated by Eq. (4.0.20).

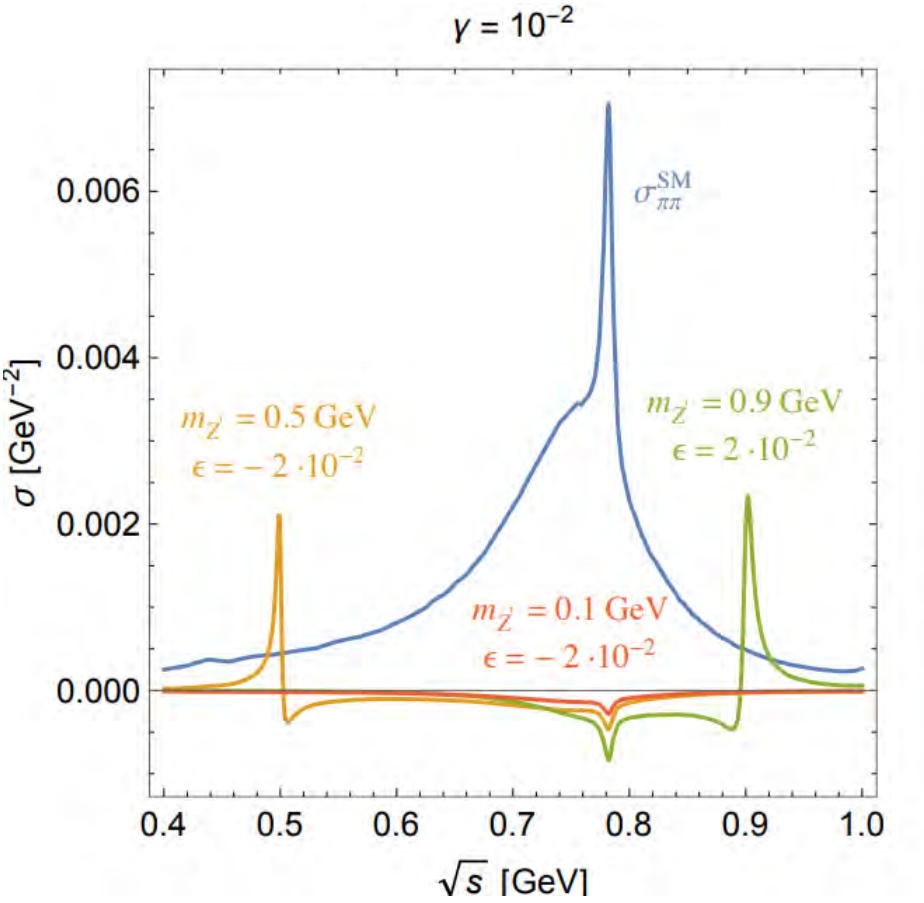

Figure 4.0.2: σ_{had}^{SM} and $\triangle\sigma_{had}^{NP}$ for some of the Z' model solving new puzzle .

Fig. 4.0.2 shows the profile of the non-standard model contribution ($\Delta\sigma_{had}^{NP}$) to hadronic cross-section and its comparison with the standard model counter part taken from [54], for selected values of the parameters in the Z' model aimed at resolving the discrepancy in Δa_μ.The examination shows that Z' masses lower than the ρ resonance are indicated, a negative value of ϵ is needed, while for Z' masses above it, a positive value of ϵ is required.

In order to get a positive value of Δa_μ, it is crucial that the interference term in Eq. (4.0.30) dominates over the resonant effect. Our research shows that the parameters necessary for the Z' model to explain the result can be separated into two regions: i) for $m_{Z'}$ values greater than or equal to 0.3 GeV, $|\varepsilon|$ is approximately 10^{-2} and γ is greater than or equal to 10^{-3}, and ii) for $m_{Z'}$ values less than or equal to $0.3GeV$, $|\varepsilon|$ is around 10^{-2} with no significant restrictions on γ.

Now the region of the Z' model's parameter space that is required to explain Δa_μ will be examined to see if experimental constraints allow it. For convenience, these can be categorized into three classes: 1. Semi-leptonic, 2. Leptonic and 3. Hadronic processes, iso-spin violating observables.

1. Semi-leptonic Processes

The cross section, represented by σ_{qq}, for the reaction e^+e^- to produce two quarks, has been accurately measured at LEP II with a precision of a few percent for $\sqrt{s} \in [130, 207]$ GeV [55]. Now we are going to find $\frac{\sigma_{qq}^{SM+NP}}{\sigma_{qq}^{SM}}$for some discussion,

$$M^{SM} = \frac{g^e g^q}{q^2} \bar{v}\gamma^\mu u \, q\gamma^\nu \bar{q}, \tag{4.0.50}$$

as $g^q = Q_q g^e$where Q_q is charge on final state quark and $g^e = e$ this implies that $g^e g^q = Q_q e^2$, photon is the propagator here,

$$M^{SM} = \frac{Q_q e^2}{q^2} \bar{v}\gamma^\mu u \, q\gamma^\nu \bar{q}, \tag{4.0.51}$$

lets $R \equiv \frac{\bar{v}\gamma u q\gamma^\nu \bar{q}}{q^2}$,

$$M^{SM} = Q_q e^2 R. \tag{4.0.52}$$

For Z' the amplitude is,

$$M^{NP} = \frac{g_V^e g_V^q}{q^2 - m_{Z'} - \iota m_{Z'} \Gamma_{Z'}} \bar{v}\gamma u \, q\gamma^\nu \bar{q}, \tag{4.0.53}$$

as $q^2 \gg m_{Z'}$so the last equation becomes,

$$M^{NP} = \frac{g_V^e g_V^q}{q^2} \bar{v}\gamma u \, q\gamma^\nu \bar{q}, \tag{4.0.54}$$

$$M^{SM+NP} = \frac{Q_q e^2}{q^2} \bar{v}\gamma u q\gamma^\nu \bar{q} + \frac{g_V^e g_V^q}{q^2} \bar{v}\gamma u q\gamma^\nu \bar{q}, \tag{4.0.55}$$

$$M^{SM+NP} = \frac{\bar{v}\gamma u q\gamma^\nu \bar{q}}{q^2} \left(Q_q e^2 + g_V^e g_V^q \right), \tag{4.0.56}$$

$$M^{SM+NP} = R \left(Q_q e^2 + g_V^e g_V^q \right), \text{ as defined } R \equiv \frac{\bar{v}\gamma u q\gamma^\nu \bar{q}}{q^2} \tag{4.0.57}$$

As cross-section σ is proportional to amplitude square,

$$\sigma^{SM+NP} = \left| R \left(Q_q e^2 + g_V^e g_V^q \right) \right|^2, \tag{4.0.58}$$

$$\sigma_{qq}^{SM} = \left| Q_q e^2 R \right|^2. \tag{4.0.59}$$

Divide Eq. (4.0.57) by Eq.(4.0.59) implies,

$$\frac{\sigma_{qq}^{SM+NP}}{\sigma_{qq}^{SM}} = \left|\frac{R\left(Q_q e^2 + g_V^e g_V^q\right)}{Q_q e^2 R}\right|^2 = \left|\frac{Q e^2 + g_V^e g_V^q}{Q_q e^2}\right|^2 = \left|1 + \frac{g_V^e g_V^q}{Q_q e^2}\right|^2, \tag{4.0.60}$$

$$\frac{\sigma_{qq}^{SM+NP}}{\sigma_{qq}^{SM}} = (1)^2 + \left(\frac{g_V^e g_V^q}{Q_q e^2}\right)^2 + 2\left(\frac{g_V^e g_V^q}{Q_q e^2}\right), \tag{4.0.61}$$

the factor $\frac{g_V^e g_V^q}{Q_q e^2}$ very small, this implies that,

$$\frac{\sigma_{qq}^{SM+NP}}{\sigma_{qq}^{SM}} \approx 1 + 2\frac{g_V^e g_V^q}{e^2 Q_q}. \tag{4.0.62}$$

The difference from unity in Eq. (4.0.62) must be smaller than 1% [55] leads to $g_V^e g_V^q \lesssim 4.6 \times 10^{-4}|Q_q|$ this implies $\epsilon \lesssim 3.3 \times 10^{-3}$.

2. Leptonic Processes.

The coupling of electrons to Z' coupling is also tightly constrained. The absence of the process where electrons and positrons collide to produce gamma rays and Z' particles that then decay into electrons and positrons at BaBar has led to an estimation that $g_V^e \lesssim 2 \times 10^{-4}$ [56], if Z' mostly decays to electrons. This constraint only holds true for Z' particles with a mass less than or equal to 0.3 GeV when the decay into pions is not possible due to kinematics. The $g_\mu - 2$ measurement provides another restriction, resulting in a limit on $|g_V^e| \lesssim 10^{-2}(m_{Z'}/0.5\,)$ GeV for $m_{Z'} \gtrsim$MeV.

3. Iso-spin Breaking Observables.

The contribution of Z' to the change in the cross section of pions, denoted by$\Delta\sigma_{\pi\pi}^{NP}$, has an $\mathcal{O}(1)$ relationship with the difference in vector couplings between up and down quarks, represented by the iso-spin breaking factor $g_V^u - g_V^d$. This is done to account for the observed change in muon anomaly Δa_μ, for Z' masses greater than or equal to 0.3 GeV. It is expected that there will be significant impacts on other hadronic observables that violate iso-spin symmetry. A relevant example is the mass difference, $\Delta m^2 = m_{\pi^+} - m_{\pi^0}^2$. Like in the QED scenario, the loop contribution fromZ' has a quadratically divergent results,

$$(\Delta m^2)_{Z'} \sim \frac{\left(g_V^u - g_V^d\right)^2}{(4\pi)^2}\Lambda_\chi^2. \tag{4.0.63}$$

The mass of theZ' boson ($m_{Z'}$) is much smaller than the cut-off scale (Λ_χ), which is approximately set to 1 GeV. As the cut-off scale increases, the contribution of Z' to the mass-squared difference (Δm^2) decouples as $\Lambda_\chi^2/m_{Z'}^2 \ll 1$. Re-scaling the prediction of SM from lattice QCD is a more practical method in practice for obtaining the NP contribution from a Z' [57] with $(g_V^u - g_V^d)^2/e^2$. Then by comparing the experimental value with the SM prediction of Δm^2, we find the 95% C.L. bound $|g_V^u - g_V^d| \lesssim 0.06$.

In Fig. 4.0.3 we display the interplay of $-g_V^e$ vs $g_V^e - g_V^d$ for two representative scenarios where $m_{Z'} = 0.1$ GeV and $m_{Z'} = 0.5$ GeV. The arrowhead directions represent the regions that were excluded by the various experimental bounds. Instead, the area favored by the explanation of the $g_\mu - 2$ discrepancy is the red band. Regardless of the Z' mass it is clear from Fig. 4.0.3 that there are always at least two separate constraints that prevent the resolution of the new $g_\mu - 2$ puzzle.

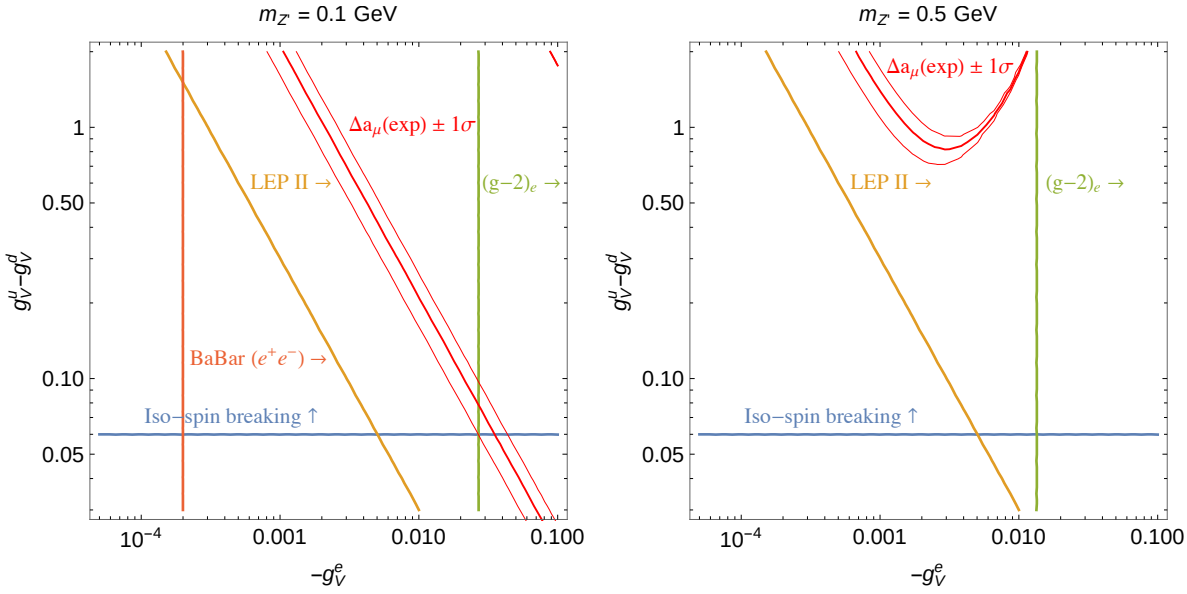

Figure 4.0.3: The impact of Z' on the discrepancy (Δa_μ) by changing the hadronic cross-section (σ_{had}), and the limitations imposed by Z' can be reevaluated.

Chapter 5

Conclusion

The BMW collaboration's recent results in lattice QCD show a discrepancy with the data used to calculate the hadronic vacuum polarization contribution to the $g_\mu - 2$. This study explored the possibility of resolving this tension, known as the new $g_\mu - 2$ puzzle, by suggesting the involvement of new physics in the hadronic cross-section σ_{had}. And propose that a negative shift in the cross-section due to new physics could restore consistency. The scenario requires the presence of a light mediator of new physics that affects the experimental cross-section σ_{had} . However, this hypothesis is not supported by several experimental findings. Additional confirmation is necessary to shed light on this puzzle, which could come from additional lattice QCD calculations or direct experimental measurements, as suggested by the MUonE experiment [58, 59, 60].

Bibliography

[1] Keshavarzi, Alex, Kim Siang Khaw, and Tamaki Yoshioka. "Muon g− 2: A review." Nuclear Physics B (2022): 115675.

[2] Abi, Babak, et al. "Measurement of the positive muon anomalous magnetic moment to 0.46 ppm." Physical Review Letters 126.14 (2021): 141801.

[3] G.W. Bennett, et al., Muon g-2 Collaboration, Final report of the Muon E821 anomalous magnetic moment measurement at BNL, Phys. Rev. D 73 (2006) 072003, arXiv:hep-ex/0602035.

[4] Aoyama, Tatsumi, et al. "The anomalous magnetic moment of the muon in the Standard Model." Physics reports 887 (2020): 1-166.

[5] M. Davier, A. Hoecker, B. Malaescu, Z. Zhang, A new evaluation of the hadronic vacuum polarisation contributions to the muon anomalous magnetic moment and to α(m2 Z), Eur. Phys. J. C 80 (3) (2020) 241, erratum: Eur. Phys. J. C 80 (5) (2020) 410, arXiv:1908.00921 [hep-ph].

[6] Aoyama, Tatsumi, et al. "The anomalous magnetic moment of the muon in the Standard Model." Physics reports 887 (2020): 1-166.

[7] Borsanyi, Sz, et al. "Hadronic vacuum polarization contribution to the anomalous magnetic moments of leptons from first principles." Physical review letters 121.2 (2018): 022002.

[8] Borsanyi, Sz, et al. "Leading hadronic contribution to the muon magnetic moment from lattice QCD." Nature 593.7857 (2021): 51-55.

[9] Di Luzio, Luca, et al. "New physics behind the new muon g-2 puzzle?." Physics Letters B 829 (2022): 137037.

[10] Gaillard, Mary K., Paul D. Grannis, and Frank J. Sciulli. "The standard model of particle physics." Reviews of Modern Physics 71.2 (1999): S96.

[11] Melnikov, Kirill, and Arkady Vainshtein. Theory of the muon anomalous magnetic moment. Vol. 216. Berlin: Springer, 2006.

[12] Carena, Marcela, et al. "MSSM Higgs boson searches at the LHC: benchmark scenarios after the discovery of a Higgs-like particle." The European Physical Journal C 73.9 (2013): 2552.

[13] Rolandi, Luigi, and Luciano Maiani. The Standard Theory of Particle Physics: Essays to Celebrate CERN's 60th Anniversary. World Scientific Publishing Co, 2016.

[14] Griffiths, D. "Introduction to Particle Physics (1987), chap. 10." nice introduction to the the ory of weak interactions: 301-309.

[15] Kobzarev, I. Yu, and L. B. Okun. "On gravitational interaction of fermions." Zh. Eksperim. i Teor. Fiz. 43 (1962).

[16] Shankar, Ramamurti. Principles of quantum mechanics. Springer Science & Business Media, 2012.

[17] Schwinger, Julian. "On quantum-electrodynamics and the magnetic moment of the electron." Physical Review 73.4 (1948): 416.

[18] Peskin, Michael E. An introduction to quantum field theory. CRC press, 2018.

[19] Aoyama, Tatsumi, et al. "The anomalous magnetic moment of the muon in the Standard Model." Physics reports 887 (2020): 1-166.

[20] Czarnecki, Andrzej, William J. Marciano, and Arkady Vainshtein. "Refinements in electroweak contributions to the muon anomalous magnetic moment." Physical Review D 67.7 (2003): 073006.

[21] Gnendiger, C., D. Stöckinger, and H. Stöckinger-Kim. "The electroweak contributions to (g− 2) μ after the Higgs-boson mass measurement." Physical Review D 88.5 (2013): 053005.

[22] Lautrup, B. E., and E. De Rafael. "Calculation of the sixth-order contribution from the fourth-order vacuum polarization to the difference of the anomalous magnetic moments of muon and electron." Physical Review 174.5 (1968): 1835.

[23] Davier, Michel, et al. "Reevaluation of the hadronic vacuum polarisation contributions to the Standard Model predictions of the muon g-2 g-2 and α (m_Z^2) using newest hadronic cross-section data." The European Physical Journal C 77 (2017): 1-12.

[24] Keshavarzi, Alexander, Daisuke Nomura, and Thomas Teubner. "Muon $g-2$ and α (M Z 2): A new data-based analysis." Physical Review D 97.11 (2018): 114025.

[25] Colangelo, Gilberto, Martin Hoferichter, and Peter Stoffer. "Two-pion contribution to hadronic vacuum polarization." Journal of High Energy Physics 2019.2 (2019).

[26] M. Davier, A. Hoecker, B. Malaescu, Z. Zhang, Reevaluation of the hadronic vacuum polarisation contributions to the Standard Model predictions of the muon g−2 and $\alpha(m_Z^2)$ using newest hadronic cross-section data, Eur. Phys. J. C77 (12) (2017) 827. arXiv:1706.09436, doi:10.1140/epjc/s10052-017-5161-6.

[27] Keshavarzi, Alexander, Daisuke Nomura, and Thomas Teubner. "Muon g− 2 and α (M Z 2): A new data-based analysis." Physical Review D 97.11 (2018): 114025.

[28] Colangelo, Gilberto, Martin Hoferichter, and Peter Stoffer. "Two-pion contribution to hadronic vacuum polarization." Journal of High Energy Physics 2019.2 (2019).

[29] Kurz, Alexander, et al. "Hadronic contribution to the muon anomalous magnetic moment to next-to-next-to-leading order." Physics Letters B 734 (2014): 144-147.

[30] Giusti, D., F. Sanfilippo, and S. Simula. "Light-quark contribution to the leading hadronic vacuum polarization term of the muon g− 2 from twisted-mass fermions." Physical Review D 98.11 (2018): 114504.

[31] Giusti, D., et al. "Electromagnetic and strong isospin-breaking corrections to the muon g− 2 from Lattice QCD+ QED." Physical Review D 99.11 (2019): 114502.

[32] Gérardin, Antoine, et al. "Leading hadronic contribution to (g− 2) μ from lattice QCD with N f= 2+ 1 flavors of O (a) improved Wilson quarks." Physical Review D 100.1 (2019): 014510.

[33] Fermilab Lattice, H. P. Q. C. D., et al. "Hadronic-vacuum-polarization contribution to the muon's anomalous magnetic moment from four-flavor lattice QCD." Physical Review D 101.3 (2020): 034512.

[34] Fujii, Keisuke, et al. "Impossibility of classically simulating one-clean-qubit model with multiplicative error." Physical review letters 120.20 (2018): 200502.

[35] Shintani, Eigo, Yoshinobu Kuramashi, and PACS Collaboration. "Hadronic vacuum polarization contribution to the muon g− 2 with (2+ 1)-flavor lattice QCD on a larger than (10 fm) 4 lattice at the physical point." Physical review D 100.3 (2019): 034517.

[36] Blum, Thomas, et al. "Calculation of the hadronic vacuum polarization contribution to the muon anomalous magnetic moment." Physical Review Letters 121.2 (2018): 022003.

[37] Borsanyi, Sz, et al. "Hadronic vacuum polarization contribution to the anomalous magnetic moments of leptons from first principles." Physical review letters 121.2 (2018): 022002.

[38] Masjuan, P., and P. Sánchez-Puertas. "Pseudoscalar-pole contribution to the $(g_\mu - 2)$: a rational approach." Phys. Rev. D 95 (2017): 054026.

[39] Masjuan, Pere, and Pablo Sanchez-Puertas. "Pseudoscalar-pole contribution to the $(g_\mu - 2)$: a rational approach." Physical Review D 95.5 (2017): 054026.

[40] Colangelo, Gilberto, et al. "Longitudinal short-distance constraints for the hadronic light-by-light contribution to $(g-2)_\mu$ with large-Nc Regge models." Journal of High Energy Physics 2020.3 (2020): 1-89.

[41] Hoferichter, Martin, et al. "Dispersion relation for hadronic light-by-light scattering: pion pole." Journal of High Energy Physics 2018.10 (2018).

[42] Roig, Pablo, and Pablo Sanchez-Puertas. "Axial-vector exchange contribution to the hadronic light-by-light piece of the muon anomalous magnetic moment." Physical Review D 101.7 (2020): 074019.

[43] Bennett, Gerald W., et al. "Final report of the E821 muon anomalous magnetic moment measurement at BNL." Physical Review D 73.7 (2006): 072003.

[44] Abi, Babak, et al. "Measurement of the positive muon anomalous magnetic moment to 0.46 ppm." Physical Review Letters 126.14 (2021): 141801.

[45] Borsanyi, Sz, et al. "Hadronic vacuum polarization contribution to the anomalous magnetic moments of leptons from first principles." Physical review letters 121.2 (2018): 022002.

[46] Borsanyi, Sz, et al. "Leading hadronic contribution to the muon magnetic moment from lattice QCD." Nature 593.7857 (2021): 51-55.

[47] Passera, M., W. J. Marciano, and A. Sirlin. "The Muon g− 2 and the bounds on the Higgs boson mass." Physical Review D 78.1 (2008): 013009.

[48] Crivellin, Andreas, et al. "Hadronic vacuum polarization:(g− 2) μ versus global electroweak fits." Physical review letters 125.9 (2020): 091801.

[49] Keshavarzi, Alexander, et al. "Muon g− 2 and Δ α connection." Physical Review D 102.3 (2020): 033002.

[50] Malaescu, Bogdan, and Matthias Schott. "Impact of correlations between a μ and α QED on the EW fit." The European Physical Journal C 81.1 (2021): 46.

[51] Colangelo, Gilberto, Martin Hoferichter, and Peter Stoffer. "Constraints on the two-pion contribution to hadronic vacuum polarization." Physics Letters B 814 (2021): 136073.

[52] Colangelo, Gilberto, Martin Hoferichter, and Peter Stoffer. "Two-pion contribution to hadronic vacuum polarization." Journal of High Energy Physics 2019.2 (2019).

[53] Schwinger, Julian. Particles, sources, and fields. CRC Press, 2018.

[54] Keshavarzi, Alexander, Daisuke Nomura, and Thomas Teubner. "g− 2 of charged leptons, α (M_Z^2), and the hyperfine splitting of muonium." Physical Review D 101.1 (2020): 014029.

[55] ALEPH Collaboration, et al. "Electroweak measurements in electron–positron collisions at W-boson-pair energies at LEP." Physics reports 532.4 (2013): 119-244.

[56] Lees, J. P., et al. "Search for a Dark Photon in e^+e^- Collisions at B a B ar." Physical review letters 113.20 (2014): 201801.

[57] Frezzotti, R., et al. "Lattice determination of the pion mass difference $M_{\pi^+} - M_{\pi^0}$ at order $\mathcal{O}(\alpha_{em})$ and $\mathcal{O}((m_d - m_u)^2)$ including disconnected diagrams." arXiv preprint arXiv:2112.01066 (2021).

[58] Calame, CM Carloni, et al. "A new approach to evaluate the leading hadronic corrections to the muon g-2." Physics Letters B 746 (2015): 325-329.

[59] Abbiendi, G., et al. "Measuring the leading hadronic contribution to the muon g-2 via μ e scattering." The European Physical Journal C 77.3 (2017): 139.

[60] Abbiendi, G. Letter of Intent: the MUonE project. No. CERN-SPSC-2019-026. 2019.

[61] Cottingham, W. Noel, and Derek A. Greenwood. An introduction to the standard model of particle physics. Cambridge university press, 2007.